Template-free Synthesis of a Macrocyclic

Bis(pyridine-dienamine) Proligand and Metal

Complexes of its Bis(pyridine-diimine) and

Bis(pyridine-dienamido) Forms

Erik D. Reinhart and Richard F. Jordan*

Department of Chemistry, The University of Chicago, 5735 South Ellis Avenue, Chicago, IL 60637, United States

KEYWORDS

Macrocyclic Ligands, Multinuclear Complexes, Template-Free Synthesis, Pyridine-diimine Complexes

ABSTRACT

We describe the template-free synthesis of the bis(pyridine-dienamine) proligand [4,5-(*m*-xylylenediamine)NH–C=(CH)(9-butyl-octahydroacridine)]₂ (2'), a variant of Burrows's macrocyclic bis(pyridine-diimine) (bis-PDI) ligand [2,6-(*m*-xylylenediamine)N=C(py)]₂ (A), using octahydroacridine as the ligand backbone. The octahydroacridine backbone favors macrocyclization by constraining the PDI units in the (s-*cis*)₂ conformation. The template-free

synthesis of 2' enables facile access to a wide array of bis-PDI and bis(pyridine-dienamido) (bis-PDE) metal complexes. Five-coordinate binuclear bis-PDI $(2)M_2Cl_4$ complexes $(2 = 4,5-(m-xylylenediamine)N=C(9-butyl-octahydroacridine)]_2$; M = Zn, Co, Fe) and a four-coordinate bis-PDI $[(2)Pd_2Br_2][B(3,5-(CF_3)_2-Ph)_4]_2$ complex were synthesized and characterized. $(2)Zn_2Cl_4$ undergoes macrocyclic ring inversion on the NMR timescale with a free-energy barrier of $\Delta G^{\neq} = 15.5(3)$ kcal/mol at 295 K. In contrast, $(2)Fe_2Cl_4$ and $(2)Co_2Cl_4$ undergo slow ring inversion on the NMR chemical shift timescale at 295 K. The amine elimination reaction of 2' with $Zr(NMe_2)_4$ yields the bis-PDE complex $(2'-4H)Zr_2(NMe_2)_4$, which was alkylated with AlMe3 and Al(CH₂SiMe₃)₃ to generate $(2'-4H)Zr_2Me_4$ and $(2'-4H)Zr_2(CH_2SiMe_3)_2(NMe_2)_2$ respectively.

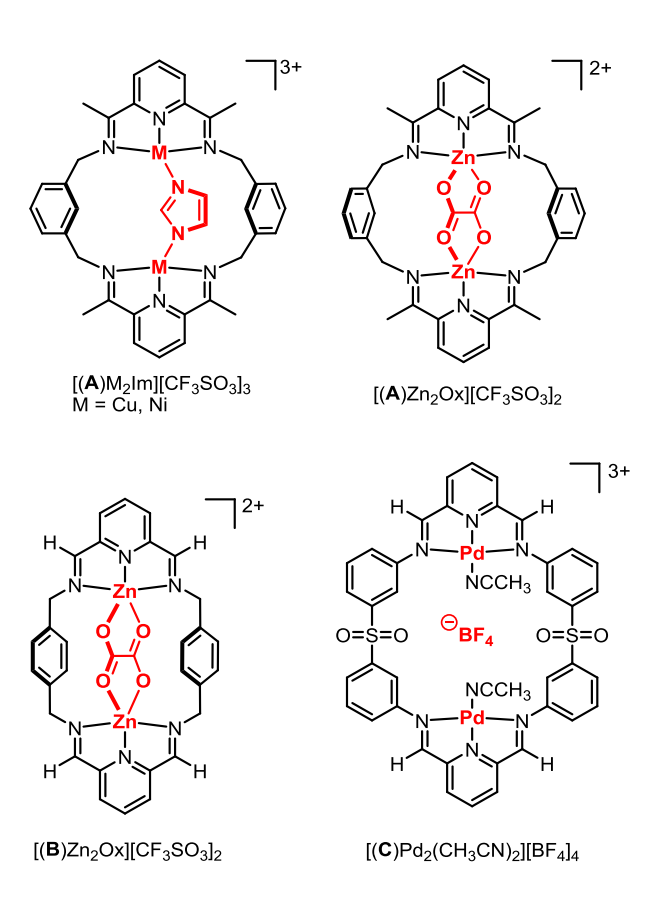
INTRODUCTION

Transition metal complexes supported by redox-active pyridine-diimine (PDI) ligands are useful catalysts for a wide range of reactions. ^{1–9} Multinuclear transition-metal complexes supported by macrocyclic bis- or multi-PDI ligands are of interest because metal-metal cooperativity effects may engender new reactivity and/or selectivity, as has been observed in other catalytic systems. ^{10–27} Several macrocyclic bis- and tris-PDI ligands have been prepared by the direct condensation of 2,6-diacetylpyridine and various dianilines. Fe and Co complexes of these ligands exhibit interesting differences in catalytic ethylene polymerization compared to analogous mononuclear complexes, although the origins of these differences remain poorly understood. ^{28–30} In general however, the attempted direct synthesis of macrocyclic multi-PDI ligands results in the formation of condensation polymer. ^{31,32} The ethylene polymerization

behavior of several metal catalysts based on discrete linear bis-PDI ligands has also been investigated.^{5,33–36}

An important strategy for avoiding the formation of linear products in the synthesis of macrocyclic ligands is the use of templates to favor macrocyclization.^{37–45} Several macrocyclic bis-PDI metal complexes have been synthesized using specially designed binucleating templates comprising two metal ions linked by an anionic bridging unit (Chart 1). Two early examples of bis-PDI complexes of this type, $[(A)M_2Im][CF_3SO_3]_3$ (M = Cu, Ni), were prepared by Burrows as models for the Ni₂ active site in urease. 46-48 These complexes were synthesized by reacting M(OTf)₂ and imidazole (ImH) to form a putative [M-Im-M]³⁺ complex, which was then added to a solution of 2,6-diacetylpyridine and m-xylylenediamine. More recently, Groysman showed that an analogous Zn complex, $[(A)Zn_2Ox][CF_3SO_3]_2$ (Ox = oxalate), is formed using in-situgenerated $[Zn_2Ox]^{2+}$ as the binucleating template.⁴⁹ The $[Zn_2Ox]^{2+}$ template also directs the condensation of 2,6-formylpyridine and p-xylylenediamine to produce $[(\mathbf{B})\mathrm{Zn_2Ox}][\mathrm{CF_3SO_3}]_2$. It should be emphasized that the binucleating templates are critical for macrocyclization in the synthesis of [(A)M₂Im][CF₃SO₃]₃ and [(A)Zn₂Ox][CF₃SO₃]₂. The attempted synthesis of these complexes in the absence of imidazole or oxalate results in intractable condensation polymers, indicating that the presence of the metal ions alone is insufficient for macrocyclization. Nitschke synthesized [(C)Pd₂(CH₃CN)₂][BF₄]₄ by the reaction of 2,6-diformylpyridine, 3-aminophenyl sulfone, and $[Pd(CH_3CN)_4][BF_4]_2$. The X-ray structure of $[(C)Pd_2(CH_3CN)_2][BF_4]_4$ shows that a BF₄ anion is located in the intermetallic cavity at a position where it can electrostatically interact with the two Pd²⁺ centers, and it was suggested by the authors that the BF₄⁻ ion functions as a template for this macrocyclization.

Chart 1. Bis-PDI Complexes Synthesized Using Binucleating Templates. Counterions are not shown.



There are two major challenges associated with using binucleating templates. First, suitable templates are difficult to design *a priori*, especially for cases involving metals with fluxional coordination geometries that result in difficult-to-predict dynamic processes for the intermediates in the condensation process. Second, the template may be difficult to remove from the product complex without destroying the macrocyclic ligand in the process. For example, Burrows found that attempted demetalation of [(A)Cu₂Im][CF₃SO₃]₃ with benzene/Na₄EDTA(aq) is inefficient due to poor solubility of the complex in organic solvents, a slow demetalation rate (even at

elevated temperatures), and a competitive rate of hydrolysis of free ligand **A**. Groysman screened various demetalation procedures and found that the removal of the Zn₂Ox²⁺ unit of [(**B**)Zn₂Ox][CF₃SO₃]₂ requires the use of strong aqueous acid, which hydrolyzes **B**. Also, while not reported by Nitschke, in our hands, attempting to demetalate [(**C**)Pd₂(CH₃CN)₂][BF₄]₄ with Na₄EDTA results in decomposition. The objective of the present work was to develop a non-templated synthesis of a variant of ligand **A** in order to enable the synthesis of a wide range of dinuclear bis-PDI complexes.

RESULTS AND DISCUSSION

Use of 9-Butyl-1,2,3,4,5,6,7,8-Octahydro-4,5-acridinedione to Favor Macrocyclization. The function of the templates in the synthesis [(A)M₂Im]²⁺, [(A)Zn₂Ox]²⁺, and [(B)Zn₂Ox]²⁺ can be understood by examining the conformations of the pyridine-diketone (PDK), pyridine-imine-ketone (PIK), and PDI units that are involved in condensation reactions leading to macrocyclization. Two limiting conformations for these units, (s-cis)₂ and (s-trans)₂, are shown in Scheme 1. While the (s-cis)₂ conformation is present in (PDI)M complexes, free PDK, PIK and PDI ligands normally adopt the (s-trans)₂ conformation because in this conformation the C=X (X = O or NR)/pyridine lone-pair repulsion that is present in the (s-cis)₂ conformation is relieved.^{28,51-56} The final intermediate in the formation of a bis-PDI macrocycle in a PDK/dianiline condensation reaction is a species that has one PIK moiety, one PDI unit and one amine group (Scheme 2). In the ground-state 2(s-trans)₂ conformer of this intermediate, the distance between the reactive ketone and amine groups is maximized and the formation of condensation polymer is favored. In the presence of a template however, the desired 2(s-cis)₂

conformation is trapped by coordination of the C=X moieties to the metal ions, and cyclization is favored.

Scheme 1. Limiting conformations of PDI, PIK and PDK compounds. X = O or NR.

Scheme 2. Conformers of the final intermediate in the formation of macrocyclic bis-PDI compounds.

One potential strategy for promoting macrocyclization in the absence of a template is to use a PDK substrate that adopts the (s-cis)₂ conformation. This was accomplished in the present work by the use of 9-butyl-1,2,3,4,5,6,7,8-octahydro-4,5-acridinedione (1, Scheme 1), in which the annulated octahydroacridine backbone (**D**, Figure 1) constrains the PDK unit to the (s-cis)₂ conformation.^{57–59}

Synthesis of Bis(pyridine-dienamine) Proligand 2'. Compound **1** was prepared using procedures reported by Bell and Thummel for similar compounds. $^{57,60-62}$ The reaction of **1** and m-xylylenediamine in butanol in the presence of p-toluenesulfonic acid yields bis(pyridine-dienamine) compound **2'**, a tautomer of bis-PDI compound **2**, in 88 % yield (Scheme 3). This condensation-macrocyclization reaction is performed at total concentration of 415 mM, 2.3 times more concentrated than the templated synthesis of $[(\mathbf{A})\mathrm{Cu}_2\mathrm{Im}][\mathrm{CF}_3\mathrm{SO}_3]_3$ (total concentration of 2,6-diacteylpyridine + m-xylylenediamine = 180 mM), underscoring the advantage of constraining the PDK moieties in the (s- $cis)_2$ conformation.

The IR spectrum of **2'** contains a characteristic N–H stretching band at 3400 cm⁻¹. The 1 H NMR spectrum of **2'** contains triplet at δ 5.11 for the N–H hydrogens, which are coupled to the benzylic hydrogens (δ 4.11), and a sharp triplet at δ 4.87 for the vinylic hydrogens, which are coupled to the neighboring methylene hydrogens on the octahydroacridine backbone. The 13 C{ 1 H} NMR spectrum of **2'** contains resonances at δ 126.7 and 98.7, which are characteristic of the vinylic carbons of an enamine. In contrast, the tetraimine tautomer **2** is expected to exhibit no IR bands above 3000 cm⁻¹, no 1 H NMR resonances in the vinylic region, no 13 C NMR resonances between δ 120 and δ 50 and a 13 C NMR resonance at ca. δ 170 for the imine carbon.

Compound 2 is disfavored due to lone-pair repulsions which are enforced by the octahydroacridine backbone. Tautomerization of 2 to 2' replaces the lone-pair repulsions with stabilizing N-H--- N_{py} hydrogen bonds between the enamine N-H and N_{py} . Thummel previously reported that condensation of non-butylated 1 with HN^iPr_2 results in the pyridine-dienamine product.

Scheme 3. Synthesis of Proligand 2'.

synthesis of a Dinuclear Bis(pyridine-diimine) Zn Complex of 2. The reaction of 2' and 2 equiv of ZnCl₂ in butanol at 110 °C for 16 h, followed by filtration and heating the resulting crude solid in CH₂Cl₂ for 2d at 35 °C generates the dinuclear bis-PDI complex (2)Zn₂Cl₄ in 60% yield (Scheme 4). The use of hot protic solvent is important as metalation is sluggish otherwise, suggesting that butanol may promote the tautomerization of 2' to 2 prior to metalation. In the solid state (2)Zn₂Cl₄ adopts a C_i-symmetric structure in which the 24-membered macrocyclic ring has a chair conformation and the geometry at the Zn centers is trigonal-pyramidal (Figure 1). The Zn1–Zn1' distance (5.515(1) Å) is significantly shorter than the Cu–Cu distance in [(A)Cu₂Im][CF₃SO₃]₃ (5.9181(9) Å) because the latter compound adopts a boat conformation enforced by the imidazolate bridge. The metrical parameters are consistent with those observed for mononuclear (PDI)ZnCl₂ complexes.^{64,65} The ¹³C{¹H} NMR spectrum of (2)Zn₂Cl₄ contains a characteristic imine carbon resonance at δ 166.3 and no resonances in the vinylic region, confirming that the macrocyclic ligand exists in the tetraimine form.

Scheme 4. Synthesis of (2)M₂Cl₄ Complexes (M = Zn, Co, Fe). Conditions: Zn: (i) BuOH, 110 °C, (ii) CH₂Cl₂. 35 °C; Co and Fe: BuOH, 110 °C.

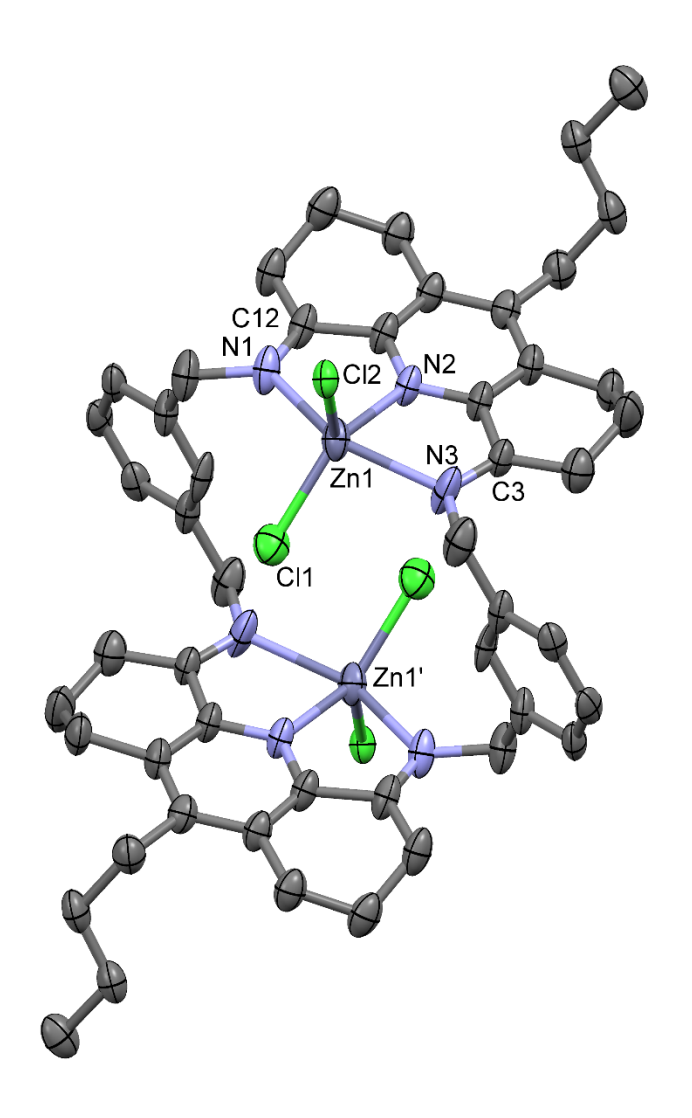


Figure 1. Molecular Structure of (2)Zn₂Cl₄•3CH₂ClCH₂Cl. H atoms, CH₂ClCH₂Cl solvent molecules and the disorder of one of the Bu groups are omitted. Key bond and atom distances (Å): N1–C12 1.284(7), N3–C3 1.308(7), Zn1–N2 2.073(4), Zn1–Cl1 2.244(1), Zn1–Cl2 2.259(1), Zn1–Zn1' 5.515(1). Key bond angles (°): N1–Zn1–N3 146.9(2), N1–Zn1–N2 73.5(2), N2–Zn1–N3 74.6(2), N3–Zn1–Cl1 135.9(1), N3–Zn1–Cl2 110.9(1). Color key: C gray, N light blue, Zn light gray, Cl green. Thermal ellipsoids are drawn at the 50% probability level.

Dynamic properties of (2)Zn₂Cl₄. The ¹H NMR spectrum of (2)Zn₂Cl₄ in CDCl₂CDCl₂ solution contains a broad AB pattern at δ 5.45 and 4.35 at 295 K for the benzylic hydrogens, which broadens further as the temperature is increased and coalesces to a broad singlet at δ 4.98 at 390 K (Figure 2, left), indicative of fluxional behavior. Lineshape analysis was performed to determine rate constants for the exchange of the benzylic hydrogens (Figure 2, right). The activation parameters determined by an Eyring analysis are Δ H[±] = 9.5(3) kcal/mol and Δ S[±] = -20.5(7) eu (see Supporting Information). The free energy barrier (Δ G[±]) is 17.0(3) kcal/mol at 366 K.

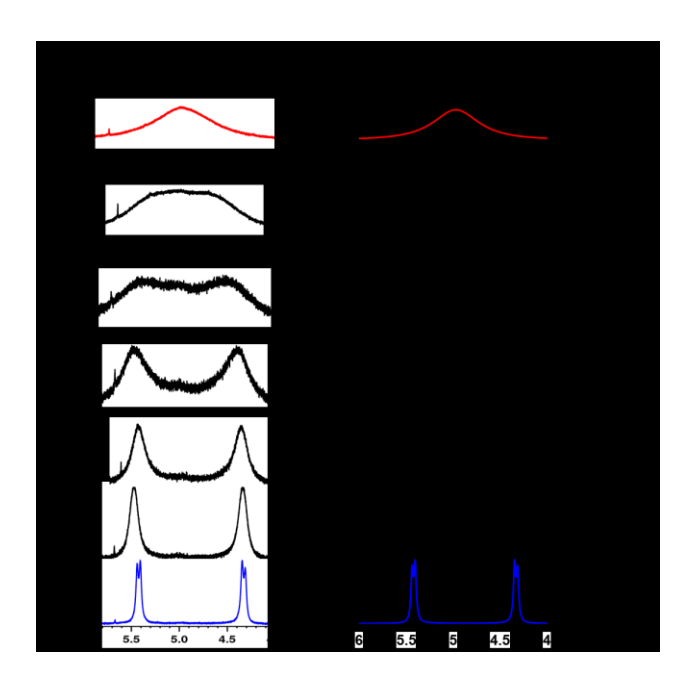


Figure 2. Benzylic hydrogen region of the variable temperature 1 H NMR spectra of (2)Zn₂Cl₄. Left: experimental spectra. Right: simulated spectra and rate constants for benzylic hydrogen exchange. NMR conditions: 500 MHz, CDCl₂CDCl₂ solution. The singlet at ca. δ 5.7 is one of the 13 C satellites of the CDCl₂CDCl₂ solvent resonance.

Additionally, the octahydroacridine methylene resonances exhibit temperature-dependent behavior (Figure 3). At 295 K, the octahydroacridine methylene hydrogens give rise to two broad resonances at δ 2.75 and 1.90, which are assigned as shown in Figure 3. As the temperature is raised, the imine α -hydrogen (H_i and H_k) resonances evolve to a broad singlet at δ 2.37 at 366 K (500 MHz) and the imine β -hydrogen (H_h and H_i) and γ -hydrogen (H_f and H_g) resonances sharpen to a quintet at δ 1.64 and a triplet at δ 2.81 respectively. The ΔG^{\neq} value estimated from the coalescence of the imine α -hydrogen resonances is 16.8(1) kcal/mol at 366 K, which is in good agreement with that determined from analysis of the benzylic hydrogen resonances 17.0(3) kcal/mol at this temperature.

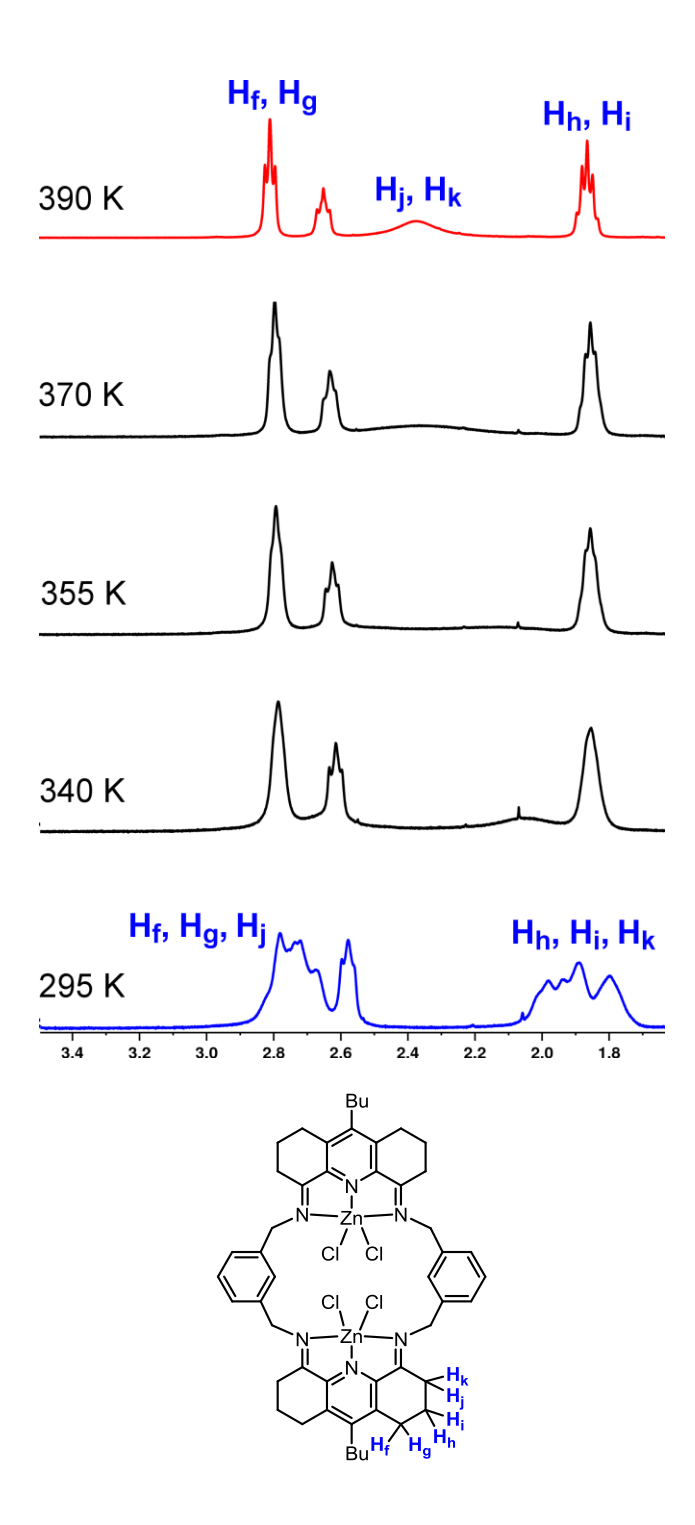


Figure 3. Top: Variable temperature behavior of the octahydroacridine ¹H NMR resonances of (2)Zn₂Cl₄. NMR conditions: 500 MHz, CDCl₂CDCl₂ solution, 295 K to 390 K. Bottom: Labelling scheme for the octahydroacridine hydrogens of (2)Zn₂Cl₄.

These results indicate that the same dynamic process permutes the benzylic hydrogens, the imine α -hydrogens, and the other octahydroacridine methylene hydrogens. The simplest such process is inversion of the 24-membered macrocyclic ring (Scheme 5). This process likely involves a series of correlated C_{xylyl} – $C_{benzylic}$ and $C_{benzylic}$ – N_{imine} bond rotations and accompanying isomerization the five-coordinate Zn centers between trigonal bipyramidal and square pyramidal geometries. The large negative ΔS^{\neq} value suggests a highly ordered transition state for this process, which results from the macrocyclic structure. Similar large negative activation entropies have observed for other compounds that undergo macrocyclic ring inversion.

Scheme 5. Macrocyclic ring inversion of (2) Zn_2Cl_4 . The blue benzylic and imine α -hydrogens occupy *exo* positions in the structure on the left and *endo* positions in the structure on the right.

Dinuclear Bis(pyridine-diimine) Co and Fe Complexes of 2. The reaction of 2' and 2 equiv of CoCl₂ in butanol at 110 °C affords (2)Co₂Cl₄, which was isolated in 80% yield (Scheme 4). The solid-state structure of (2)Co₂Cl₄ contains two independent molecules in the asymmetric unit, in both of which the macrocyclic ligand adopts chair conformation similar to that in (2)Zn₂Cl₄. In the C_i -symmetric molecule of (2)Co₂Cl₄ (C_i -(2)Co₂Cl₄, Figure 4), the Co centers

have distorted square pyramidal geometry with a Co3–Co3' distance of 5.501(1) Å. In the C_1 -symmetric molecule (C_1 -(2)Co₂Cl₄, Figure 5), there are three CH₂ClCH₂Cl solvent molecules are hydrogen bonded to the chloride ligands of Co2, and the Co1–Co2 distance is contracted to 5.304(1) Å.

The spin-only value for the magnetic moment ($\mu_{S.O.}$) of a dinuclear metal complexes with non-interacting metal centers is given by Equation 1

$$\mu_{S.O.} = 2\sqrt{S_1(S_1+1) + S_2(S_2+1)} \tag{1}$$

where S_1 and S_2 are the respective spin states of the two metal centers. ^{69,70} The μ_{eff} value for (2)Co₂Cl₄ determined by the Evans method is 6.3 BM which is consistent with two independent high-spin ($S_1 = S_2 = 3/2$) Co²⁺ centers ($\mu_{S.O.} = 5.5$ BM, Equation 1). The high-spin value of S = 3/2 and a μ_{eff} value slightly larger than $\mu_{S.O}$ is consistent with previous results for mononuclear (PDI)CoX₂ (X = Cl, Br) compounds.³ The ¹H NMR spectrum of (2)Co₂Cl₄ contains both broad and sharp paramagnetically-shifted resonances. The sharp resonances are assigned to the butyl group and the *m*-xylylenediamine linker hydrogens due to their large distance from the Co centers. The spectrum contains 14 resonances (one pair of actidine resonances are coincident) at room temperature indicating that the ring inversion for (2)Co₂Cl₄ is slow on the chemical shift time scale. 15 resonances are expected if the macrocyclic ring inversion is slow and 11 are expected if the inversion is fast.

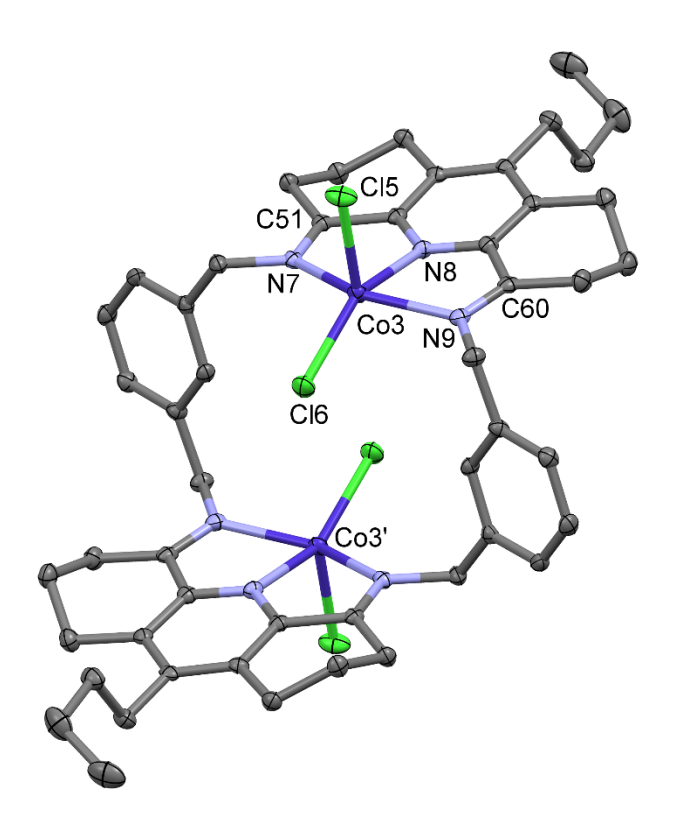


Figure 4. Molecular structure of C_i -(2)Co₂Cl₄ molecule in the asymmetric unit of 3(2)Co₂Cl₄•4CH₂ClCH₂Cl. H atoms and CH₂ClCH₂Cl molecules are omitted. Key bond and atom distances (Å): C51–N7 1.282(4), C60–N9 1.281(4), Co3–N8 2.037(3), Co3–N7 2.145(3), Co3–N9 2.189(2), Co3–Cl6 2.249(1), Co3–Cl5 2.320(1), Co3–Co3' 5.501(1). Key bond angles (°): N7–Co3–N9 148.8(1), N7–Co3–N8 75.6(1), Cl6–Co3–Cl5 114.44(4), N8–Co3–Cl6 149.55(8), N8–Co3–Cl5 95.91(8). Color key: C gray, N light blue, Co blue, Cl green. Thermal ellipsoids are drawn at 50%.

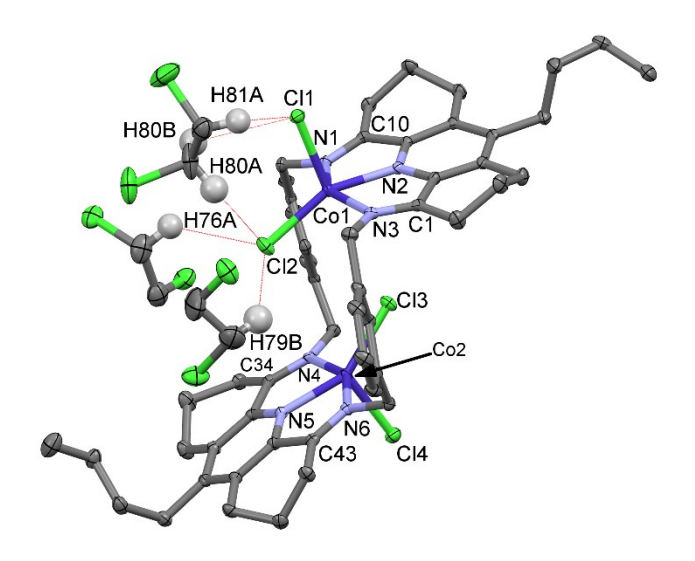


Figure 5. Molecular structure of C_1 -(2) C_0 2 Cl_4 in the asymmetric unit of

3(2)Co₂Cl₄•4CH₂ClCH₂Cl. Non-interacting CH₂ClCH₂Cl molecules and non-interacting H atoms are omitted. Hydrogen bonds are draw in red. Key bond and atom distances (Å): C10–N1 1.285(4), C60–N3 1.273(4), C34–N4 1.281(4), C43–N6 1.278(4), Co1–N2 2.033(2), Co1–N1 2.200(3), Co1–N3 2.173(3), Co1–Cl1 2.3293(9), Co1–Cl2 2.268(1), Co2–Cl3 2.2695(9), Co2–Cl4 2.3073(9), Co1–Co2 5.344(1), H81A–Cl1 2.943, H80B–Cl1 2.9291, H80A–Cl2 2.948, H79B–Cl2 2.773, H76A–Cl2 2.792. Key bond angles (°): N1–Co1–N2 74.7(1), N2–Co1–N3 75.0(1), N2–Co1–Cl1 98.95(8), N2–Co1–Cl2 152.95(8), N4–Co2–N5 75.5(1). N5–Co2–N6 75.5(1), N5–Co2–Cl3 148.73(8), N5–Co2–Cl4 97.73(8). Color key: C gray, N light blue, Co blue, Cl green. Thermal ellipsoids are drawn at 50%.

Similarly, the reaction of 2' with 2 equiv of FeCl₂ in butanol at 110 °C affords (2)Fe₂Cl₄, which was isolated in 88% yield (Scheme 4). The μ_{eff} value determined by the Evans method is 7.1 BM ($\mu_{S.O.} = 6.9$ BM, Equation 1), which is consistent with two independent high-spin (S = 2) Fe²⁺ centers and in line with data for other (PDI)FeX₂ (X = Cl, Br) complexes.³ The ¹H NMR

spectrum contains 15 resonances, indicative of slow ring inversion on the NMR chemical shift time scale.

Synthesis of a Dinuclear Bis(pyridine-diimine) Pd Complex of 2. The reaction of 2' with 4 equiv of PdBr₂ in CH₃CN yields a brown precipitate, tentatively assigned as [(2)Pd₂Br₂][Pd₂Br₆] (Scheme 6). This assignment is based on the reported reaction of PDI^{Ph} (N,N-(2,6pyridinediyldiethylidyne)bis-benzenamine) and PdCl₂ to produce [(PDI^{Ph})PdCl][PdCl₃],^{71–74} and crystallographic evidence that shows that PdBr₃- exists as the Pd₂Br₆²- dimer. 75-77 [(2)Pd₂Br₂][Pd₂Br₆] was not characterized due to poor solubility but rather was converted to $[(2)Pd_2Br_2][BAr^F_4]_2$ by anion exchange using NaBAr^F₄ (Ar^F = 3,5-(CF₃)₂-Ph) in 63 % overall yield from 2' and PdBr₂. The solid state structure of [(2)Pd₂Br₂][BAr^F₄]₂ is shown in Figure 5. The conformation of the bis-PDI ligand is similar to that in (2) Zn_2Cl_4 , C_i -(2) Co_2Cl_4 , and C_1 -(2)Co₂Cl₄ with the complex adopting a C_i-symmetric structure with a Pd1-Pd1' distance of 4.9402(4) Å, shorter than the M-M distances in (2)Zn₂Cl₄ and (2)Co₂Cl₄. The Pd centers are square planar and the bromine atoms are positioned directly over the axial site of the distal Pd center at a distance of 4.0336(4) Å. This distance is larger than the sum of Van der Waals radii of Pd and Br (3.48 Å) ruling out any significant bonding interaction, but the contracted N2-Pd1-Br1 angle (174.71(6)°) suggests that a weak electrostatic interaction may be present. The ¹H NMR spectrum of [(2)Pd₂Br₂][BAr^F₄]₂ contains broad signals for the benzylic and octahydroacridine methylene hydrogens, suggesting that macrocyclic ring inversion is occurring on the NMR time scale as observed for (2)Zn₂Cl₄. However, $[(2)Pd_2Br_2][BAr^F_4]_2$ is not stable above room temperature and therefore VT NMR analysis was not possible.

Scheme 6. Synthesis of $[(2)Pd_2Br_2][BAr^F_4]_2$ ($Ar^F = 3,5-(CF_3)_2-Ph$).

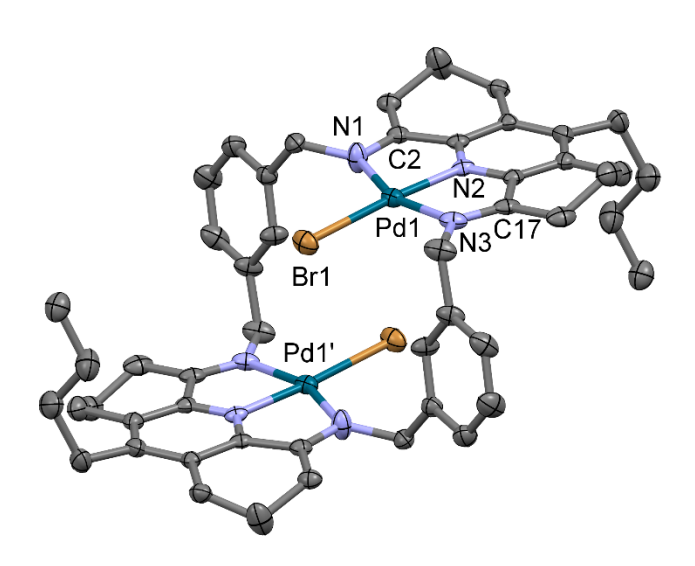


Figure 6. Molecular structure of [(2)Pd₂Br₂][BAr^F₄]₂. H atoms and BAr^F₄ anions are omitted. Key bond and atom distances (Å): N1–C2 1.334(4), N3–C17 1.299(4), Pd1–N1 2.061(2), Pd1–N3 2.054(2), Pd1–N2 1.929(2), Pd1–Br1 2.4009(4), Pd1–Pd1 4.9402(4), Pd1 –Br1 4.0336(4). Key bond angles (°): N1–Pd1–N2 80.07(9) N2–Pd1–N3 79.48(9), N1–Pd1–N3 159.14(9), N1–Pd1–Br1 99.15(7), N3–Pd1–Br1 101.59(6), N2–Pd1–Br1 174.71(6). Color key: C gray, N light blue, Pd teal, Br orange. Thermal ellipsoids are drawn at 50%.

Synthesis of Bis(pyridine-enamido) Zr Complexes. The reaction of **2'** with 2 equiv of Zr(NMe₂)₄ in PhCl affords (**2'**–4H)Zr₂(NMe₂)₄ in 79 % yield via amine elimination (Scheme 7). Alkylation reactions of (**2'**–4H)Zr₂(NMe₂)₄ were explored in an effort to prepare a crystalline analogue for structural analysis (Scheme 8). (**2'**–4H)Zr₂(NMe₂)₄ reacts with excess AlMe₃ to produce (**2'**-4H)Zr₂Me₄ in 67 % yield and with Al(CH₂SiMe₃)₃ to afford (**2'**–4H)Zr₂(CH₂SiMe₃)₂(NMe₂)₂ in 74 % yield.

Scheme 7. Synthesis of (2'-4H)Zr₂(NMe₂)₄.

The ¹H and ¹³C{¹H} NMR spectra of (2'-4H)Zr₂(NMe₂)₄, (2'-4H)Zr₂Me₄ and (2'-4H)Zr₂(CH₂SiMe₃)₂(NMe₂)₂ contain characteristic vinylic resonances at δ 4.6 - 4.8 and δ 98 - 100 for the PDE ligand. Additionally, the ¹H NMR spectra contain sharp AB patterns for the benzylic hydrogens, indicative of static structures in solution. The ¹H NMR spectrum of (2'-4H)Zr₂(CH₂SiMe₃)₂(NMe₂)₂ does not broaden as the temperature is increased and no EXSY correlations between the benzylic resonances are observed in the ¹H-¹H NOESY spectrum. Pidonation from the enamido and amido ligands into the *d*⁰ Zr centers may contribute to the rigidity of the bis-PDE complexes.

Scheme 8. Synthesis of (2'-4H)Zr₂Me₄ and (2'-4H)Zr₂(CH₂SiMe₃)₂(NMe₂)₂.

X-ray analysis of (2'-4H)Zr₂(CH₂SiMe₃)₂(NMe₂)₂ shows two independent *C_i* symmetric molecules in the asymmetric unit which differ primarily in the angles between the -NMe₂ groups and the pyridine planes. In one of these molecules, *perp*-(2'-4H)Zr₂(CH₂SiMe₃)₂(NMe₂)₂ (Figure 7) the -NMe₂ groups have an angle of 86.25° to the pyridine ring while the other, *skewed*-(2'-4H)Zr₂(CH₂SiMe₃)₂(NMe₂)₂, exhibits a smaller angle of 72.34° (see Supporting Information). The macrocyclic ligands in both molecules adopts a chair conformation similar to those in the aforementioned bis-PDI complexes. The Zr centers exhibit distorted square-pyramidal geometries with the bulky -CH₂SiMe₃ groups in the more sterically-accessible axial sites, and the

smaller -NMe₂ groups in the equatorial sites. In *perp*-(2'-4H)Zr₂(CH₂SiMe₃)₂(NMe₂)₂ the C-N (ave. 1.391[5] Å) and C-C (ave. 1.348[5] Å) bond distances of the enamido functional groups are characteristic of a C-N single bond and a C-C double bond respectively, and are consistent with data for previously reported PDE metal complexes.⁷⁸⁻⁸⁰ Similar bond distances are observed in *skewed*-(2'-4H)Zr₂(CH₂SiMe₃)₂(NMe₂)₂. The metal-metal distances in *perp*-(2'-4H)Zr₂(CH₂SiMe₃)₂(NMe₂)₂ and *skewed*-(2'-4H)Zr₂(CH₂SiMe₃)₂(NMe₂)₂ are elongated to 6.1273(7) Å and 5.8553(6) Å respectively, significantly longer than those in (2)Zn₂Cl₄, (2)Co₂Cl₄, and [(2)Pd₂Br₂][BAr^F₄]₂.

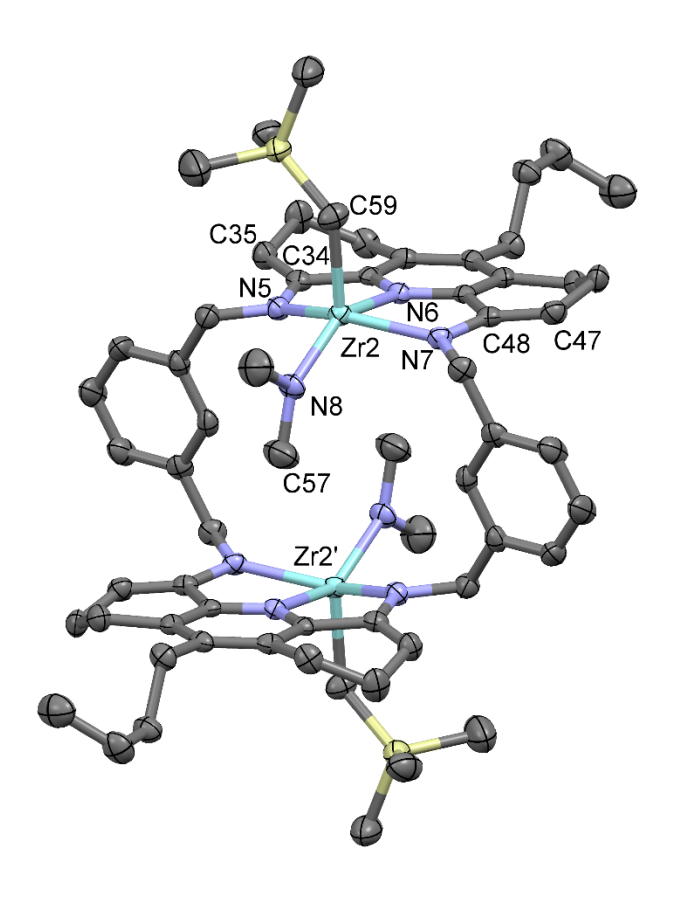


Figure 7. Molecular structure of *perp*-(2'-4H)Zr₂(CH₂SiMe₃)₂(NMe₂)₂. H atoms are omitted. Key bond and atom distances (Å): N5–C34 1.391(4), N5–C48 1.390(3), C34–C35 1.347(4),

C48–C47 1.349(3), N5–Zr2 2.151(2), N6–Zr2 2.248(2), N7–Zr2 2.149(2), C59–Zr2 2.240(3), N8–Zr2 2.050(2), Zr2–Zr2' 6.1273(7). Key bond angles (°): N5–Zr2–N6 70.25(9), N6–Zr2–N7 69.97(9), N6–Zr2–C59 101.4(1), N6–Zr2–N8 143.83(9), N5–Zr2–N8 98.38(9). Color key: C gray, N light blue, Zr cyan, Si tan. Thermal ellipsoids are drawn at 75%.

CONCLUSION

The reaction of 1 and m-xylylenediamine affords macrocyclic bis(pyridine-dienamine) proligand 2' in high yield in the absence of a binucleating template. The octahydroacridine backbone constrains 1 and analogous pyridine-imine-ketone species to the (s-cis)₂ conformation, which favors macrocyclization over the formation of linear condensation polymers. 2' reacts with MX₂ salts via tautomerization and metalation to form bis-PDI complexes, including fivecoordinate (2) M_2Cl_4 (M = Zn, Co, Fe) complexes and a 4-coordinate [(2) Pd_2Br_2][BAr^F₄]₂ complex. 2' reacts with Zr(NMe₂)₄ via amine elimination to form the bis-PDE complex (2'-4H)Zr₂(NMe₂)₄, which is alkylated by AlMe₃ and Al(CH₂SiMe₃)₃ to generate (2'-4H)Zr₂Me₄ and $(2'-4H)Zr_2(CH_2SiMe_3)_2(NMe_2)_2$. X-ray structural analyses of $(2)M_2Cl_4$ (M = Zn, Co), $[(2)Pd_2Br_2][BAr^F_4]_2$ and $(2'-4H)Zr_2(CH_2SiMe_3)_2(NMe_2)_2$ show that the bis-PDI ligand 2 and bis-PDE ligand [2'-4H]⁴⁻ adopt chair conformations and are sufficiently flexible to accommodate trigonal bipyramidal, square planar and square pyramidal geometries at the metal centers. (2)Zn₂Cl₄ undergoes macrocyclic ring inversion in solution with a free energy barrier of ΔG^{\neq} = 17.0(3) kcal/mol at 380 K. The large negative ΔS^{\neq} of -20.5(7) for this unimolecular process is indicative of a highly correlated transition state. Line broadening in the ¹H NMR spectrum of [(2)Pd₂Br₂][BAr^F₄]₂ is indicative of a similar macrocyclic ring inversion process. Ring inversion

is slow on the NMR chemical shift timescale for $(2)M_2Cl_4$ (M = Co, Fe) and the three bis-PDE Zr₂ complexes.

EXPERIMENTAL SECTION

General Procedures. All experiments were performed using drybox or Schlenk techniques under a nitrogen atmosphere unless noted otherwise. Nitrogen was purified by passage through Q-5 oxygen scavenger and activated molecular sieves. CH₂Cl₂, Et₂O, THF were dried by passage through activated alumina. Hexanes and pentanes were purified by passage through BASF R3-11 oxygen scavenger and activated alumina. CH₂ClCH₂Cl was dried over MgSO₄ for 24 h and then distilled over calcium hydride and stored under nitrogen. CDCl₃, CD₂Cl₂, CDCl₂CDCl₂, and C₆D₅Cl were distilled from and stored over activated 3 Å molecular sieves. C₆D₆ and C₆D₅CD₃ were distilled from Na/benzophenone. Anhydrous metal salts were purchased from Strem Chemical, Inc. and used without further purification. Acetic acid, benzaldehyde, anhydrous acetonitrile, anhydrous butanol, and AlMe₃ were purchased from Sigma-Aldrich and used without further purification. m-Xylylenediamine was purchased from Sigma-Aldrich, distilled, and stored under nitrogen. NaBArF₄ (ArF= 3,5-(CF₃)₂-Ph) was donated by Boulder Scientific and used as received. Elemental analyses were performed by Midwest Microlab. 9butyl-1,2,3,4,5,6,7,8-octahydroacridine was synthesized using the procedure reported by Bell. 60,61 Al(CH₂SiMe₃)₃ was synthesized according to literature procedures. 81

NMR spectra were recorded on a Bruker ADVANCE II+ 500 or DRX 400 spectrometer at room temperature unless otherwise specified. 1 H and 13 C chemical shifts are reported relative to SiMe₄ and internally referenced to residual 1 H and 13 C solvent resonances. 11 B and 19 F chemical shifts were externally referenced to BF₃OEt₂ (δ 0.0 for 11 B and δ –153.0 for 19 F).

Electrospray mass spectra (ESI-MS) were recorded on an Aglient 6130 LCMS (low resolution) instrument. High-resolution accurate mass spectra (HRA-MS) were recorded on an Agilent 6224 TOF-MS instrument in mixed mode. MALDI-TOF-TOF-MS spectra were collected on a Bruker Ultraflextreme instrument using dithranol as the matrix. The observed isotope patterns closely matched isotope patterns calculated using envipat 2.2 Web,⁸² and are reported in the SI for each metal complex. The reported m/z value corresponds to the most intense peak in the isotope pattern.

X-ray quality crystals of (2)Zn₂Cl₄, (2)Co₂Cl₄, and [(2)Pd₂Br₂][BAr^F₄]₂ were grown by

diffusion of hexanes into a 1,2-dichloroethane solution of each compound (1/1) at room temperature over 2 days. X-ray quality crystals of (2'-4H)Zr₂(CH₂SiMe₃)₂(NMe₂)₂ were grown by diffusion of hexanes into a saturated toluene solution (15/1) at room temperature over 3 days. 9-Butyl-1,2,3,4,5,6,7,8-octahydro-4,5-bis(phenylmethylene)-acridine (Scheme 9). 9-butyl-1,2,3,4,5,6,7,8-octahydroacridine (39.2 g, 0.161 mol) and acetic anhydride (120 mL, 1.27 mol) were added to a round bottom flask. Benzaldehyde (145 mL, 1.43 mmol) was added using an addition funnel. The orange solution was refluxed for 16 h, during which time the solution turned a dark red color. The flask was submerged in an ice bath until a yellow crystalline solid began to form and was then transferred to a -15 °C freezer and left to stand for 6 h. The resulting yellow crystalline solid was collected by filtration and washed with ethanol (3 x 150 mL). The solid was dried overnight under 9-butyl-1,2,3,4,5,6,7,8-octahydro-4,5vacuum to yield bis(phenylmethylene)-acridine as a yellow crystalline solid. Yield: 54.0 g, 83 %. By ¹H NMR, the major impurities are benzaldehyde, acetic acid, and acetic anhydride. ¹H NMR (CDCl₃, 500 MHz): δ 8.11 (s, 2H, PhHC=C), 7.42 (d, ${}^{3}J_{HH}$ = 10 Hz, 4H, o-Ar), 7.35 (t, ${}^{3}J_{HH}$ = 10 Hz, 4H, m-Ar), 7.22 (t, ${}^{3}J_{HH} = 10 \text{ Hz}$, 2H, p-ArH), 2.83 (m, 8H, C=CC H_{2} CH₂CH₂CH₂), 2.59 (t, ${}^{3}J_{HH} = 10 \text{ Hz}$,

2H, $CH_2CH_2CH_3$), 1.84 (quintet, ${}^3J_{HH} = 5$ Hz, 4H, $C=CCH_2CH_2CH_2$), 1.44 (m, 4H, $CH_2CH_2CH_2CH_3$), 0.97 (t, ${}^3J_{HH} = 9$ Hz, 3H, $CH_2CH_2CH_2CH_3$). ${}^{13}C\{{}^{1}H\}$ NMR (CDCl₃, 500 MHz): δ 149.6, 148.4, 138.6, 136.8, 129.8, 129.6, 128.1, 126.5, 126.3, 30.7, 28.2, 27.8, 26.4, 23.5, 23.2, 14.0. ESI-MS m/z: 420.3 [M+H]⁺. ESI/APCI-TOF HR-MS (m/z): [M+H]⁺. Calcd for $C_{31}H_{33}N$ 420.2686; Found 420.2691.

Scheme 9. Synthesis of 9-butyl-1,2,3,4,5,6,7,8-octahydro-4,5-bis(phenylmethylene)-acridine.

$$\begin{array}{c} \begin{array}{c} \\ \\ \\ \\ \\ \\ \\ \\ \\ \\ \\ \end{array} \end{array}$$

9-Butyl-1,2,3,4,5,6,7,8-octahydro-4,5-acridinedione (1. Scheme 10). A three-neck round bottom flask connected to an O₂ line with an electrolytic ozone generator was charged with 9-butyl-1,2,3,4,5,6,7,8-octahydro-4,5-bis(phenylmethylene)-acridine (11.2 g, 26.7 mmol), CH₂Cl₂ (300 mL), and methanol (100 mL). The flask was cooled to -78 °C while O₂ was bubbled through the solution. The flask was connected to a bubbler containing a 10% solution of KI in 1/1 water/acetic acid (O₃ indicator solution). The solution was sparged with O₂ for 15 min and the electrolytic ozone generator was turned on. After 45 min to 1 h, the solution had a persistent blue color. The generator was turned off and the solution was purged with O₂ for 15 min, resulting in a colorless solution. Dimethyl sulfide (9 mL, 0.12 mol) was added dropwise, and the resulting pale-yellow solution was stirred for 16 h at room temperature. The resulting bright yellow solution was concentrated to a yellow oil under vacuum and washed with hot hexane (2 x 40

mL). The oil was dissolved in CH₂Cl₂ (100 mL) and washed with water (40 mL), 15 % aqueous sodium bisulfite (50 mL), and water (40 mL). The organic layer was dried with MgSO₄ and concentrated on a rotary evaporator. The resulting yellow oil was triturated with Et₂O (100 mL) and vigorously stirred to yield a bright yellow solid, which was collected by filtration and washed with Et₂O (2 x 25 mL). The solid was ground in a mortar and pestle and placed in a vacuum oven at 70 °C overnight, to yield 1 as a yellow solid. Yield: 4.7 g, 72 %. ¹H NMR: (CDCl₃, 500 MHz): δ 3.03 (t, ³*J*_{HH} = 6.5 Hz, 4H, O=CCH₂CH₂CH₂), 2.79 (dd, ³*J*_{HH} = 7.5 Hz, ³*J*_{HH} = 6 Hz, 4H, O=CCH₂CH₂CH₂), 2.73 (t, ³*J*_{HH} = 8 Hz, 2H, CH₂CH₂CH₂CH₃), 2.19 (quintet, ³*J*_{HH} = 6.5 Hz, 4H, O=CCH₂CH₂CH₂), 1.48 (m, 4H, CH₂CH₂CH₂CH₃), 0.99 (t, ³*J*_{HH} = 7 Hz, 3H, CH₂CH₂CH₂CH₃). ¹³C{¹H} NMR (CDCl₃, 125 MHz): δ 196.1, 150.7, 147.1, 141.5, 39.2, 30.5, 28.5, 26.2, 23.2, 21.9, 13.8. ESI-MS (m/z): 272.2 [M+H]⁺. ESI/APCI-TOF HR-MS (m/z): [M+H]⁺ Calcd for C₁₇H₂₂NO₂ 272.1645; Found 272.1651.

Scheme 10. Synthesis of 1.

2'. A flask was charged with 1 (1.69 g, 6.23 mmol), *p*-toluenesulfonic acid hydrate (59 mg, 0.62 mmol), and n-butanol (30 mL), and the mixture was stirred at room temperature until it became homogeneous. *m*-Xylylenediamine (848 μL, 6.23 mmol) was added via syringe. A beige precipitate began to form within 5 min. The dark red reaction mixture was stirred for 1 h. The resulting beige precipitate was collected by filtration and washed with ethanol (125 mL) under air and dried under vacuum overnight to yield 2' as a beige solid Yield: 1.90 g, 82 %. The atom

labelling scheme for **2'** is shown in Figure 8. ¹H NMR (CDCl₃, 500 MHz): δ : 7.30 (m, 8H, H_c, H_d, H_e), 5.01 (br t, ${}^{3}J_{HH} = 4H$, H_j), 4.92 (t, ${}^{3}J_{HH} = 4.5$ Hz, 4H, H_k), 4.09 (d, ${}^{3}J_{HH} = 4$ Hz, 8H, H_a,H_b), 2.81 (t, ${}^{3}J_{HH} = 8$ Hz, 8 H, H_f,H_g), 2.65 (t, ${}^{3}J_{HH} = 7.5$ Hz, 4H, H_l), 2.37 (q, ${}^{3}J_{HH} = 4.5$ Hz, 8H, H_h,H_i), 1.43 (m, 8H, H_m, H_n), 0.95 (t, ${}^{3}J_{HH} = 6$ Hz, 6H, H_o). ${}^{13}C\{{}^{1}H\}$ NMR (CDCl₃, 126 MHz): δ 145.8 (*o*-py), 145.4 (*m*-py), 141.2 (*p*-py), 139.9 (C_{xylyl} -C_{benzylic}), 129.3 (N-C=C), 129.2 (C-H_c, C-H_d, or C-H_e), 128.6 (C-H_c, C-H_d, or C-H_e), 126.7 (C-H_c, C-H_d, or C-H_e), 94.8 (C-H_k), 48.8 (C-H_a,H_b), 31.8 (C-H_m), 28.3 (C-H_l), 24.5 (C-H_f, H_g), 23.1 (C-H_n), 21.9 (C-H_h,H_i), 14.1 (C-H_o). IR (KBr Disk): v(cm⁻¹) 3400.2 (N-H), 3049.4, 2955.0, 2874.0, 2854.1, 2812.2, 1641.6, 1560.2, 1488.5, 1464.5, 1427.8, 1403.6, 1384.8, 1357.7, 1291.3, 1211.5, 1163.5, 1099.4, 1018.5, 978.3, 909.1, 201.5, 755.1, 703.9. ESI-MS (m/z): 743.6 [M+H]⁺, 798.3 [M+Na]⁺. ESI/APCI-TOF HRA-MS (m/z): [M+H]⁺.Calcd for C_{50} H₅₉N₆ 743.4801; Found 743.4782.

Figure 8. Labelling scheme for 2'.

(2)Zn₂Cl₄. ZnCl₂ (146.8 mg, 1.0766 mmol) and 2' (400.0 mg, 0.5383 mmol) were suspended in n-butanol (40 mL). The bright yellow suspension was heated to 110 °C and stirred for 16 h.

The yellow solid was collected and dissolved in anhydrous CH₂Cl₂ (25 mL) and heated at 35 °C for 2 d. The solution was layered with hexane (25 mL) to yield (2)Zn₂Cl₄ as a white solid, which was collected by filtration and dried under vacuum. Yield: 340 mg, 62%. The labelling scheme for (2)Zn₂Cl₄ is shown in Figure 9. ¹H NMR (CD₂Cl₂, 500 MHz): δ 8.07 (s, 2H, H_c), 7.22 (m, 6H, H_d , H_e), 5.45 (br d, $^2J_{HH}$ = 9 Hz, 4H, H_a), 4.35 (br d, $^2J_{HH}$ = 9 Hz, 4H, H_b), 2.84 (m, 12H, H_f , H_g , H_k), 2.67 (t, ${}^3J_{HH} = 7$ Hz, 4H, H_l), 1.99 (m, 12H, H_h , H_i , H_i), 1.44 (m, 8H, H_m , H_n), 0.96 (t, $^{3}J_{HH} = 7 \text{ Hz}, 6H, H_{0}$). $^{1}H \text{ NMR (CDCl}_{2}\text{CDCl}_{2}, 400 \text{ MHz}$): δ 7.99 (s, 2H), 7.15 (m, 6H), 5.42 (br d, ${}^{2}J_{HH} = 12 \text{ Hz}$, 4H), 4.33 (br d, ${}^{2}J_{HH} = 12 \text{ Hz}$, 4H), 2.78 (m, 12H), 2.58 (t, ${}^{3}J_{HH} = 8 \text{ Hz}$, 4H), 1.89 (m, 12H), 1.32 (m, 8H), 0.86 (t, ${}^{3}J_{HH} = 7$ Hz, 6H) ${}^{13}C\{{}^{1}H\}$ NMR (CD₂Cl₂, 125 MHz) δ 166.3 (C=N), 154.6 (p-py), 142.6 (o-py), 140.0 (C_{xylyl} - $C_{benzylic}$), 137.8 (m-py), 130.3 (C- H_c), 127.5 (C-H_d or C-H_e), 127.3 (C-H_d or C-H_e), 53.3 (C-H_a,H_b), 30.6 (C-H_m), 29.0 (C-H_l), 28.9 $(C-H_h,H_i)$, 25.0 $(C-H_f,H_g)$, 23.6 $(C-H_n)$, 21.2 $(C-H_h,H_i)$, 13.9 $(C-H_o)$. IR (KBr Disk): $v(cm^{-1})$ 3043.8, 2952.2, 2868.0, 1645.6, 1606.6, 1606.8, 1574.5, 1507.2, 1487.2, 1453.4, 1423.3, 1320.7, 1267.6, 1234.7, 1145.9, 1104.0, 1078.5, 1040.6, 999.8, 967.1, 935.6, 904.1, 875.6, 850.8, 784.9, 710.2. MALDI-TOF-TOF (Dithranol) (m/z): 1129.4 [M – 3Cl + Dithranol – 2H]⁺, 979.24 [M – C1⁺, 945.26 [M – 2C1]⁺, 841.37 [M – Zn – 3C1]⁺. ESI/APCI-TOF HRA-MS (m/z): [M-C1]⁺ Calcd for C₅₀H₅₈N₆Zn₂Cl₃⁺ 979.2323; Found 979.2314.

Figure 9. Labelling scheme for (2) M_2Cl_4 (M = Zn, Co, Fe).

(2)Co₂Cl₄. CoCl₂ (139.8 mg, 1.077 mmol) and 2° (400.0 mg, 0.5383 mmol) were suspended in n-butanol (40 mL). The blue suspension was heated to 110 °C and stirred for 16 h, resulting in a brown solution. The solvent was evaporated and the crude solid suspended in Et₂O (10 mL). The crude solid was then collected by filtration, washed with THF (25 mL), and dried under vacuum to afford (2)Co₂Cl₄ as a brown solid. Yield: 400 mg, 80%. The labelling scheme for (2)Co₂Cl₄ is shown in Figure 9. ¹H NMR (CD₂Cl₂, 500 MHz, 23 °C): δ 62.71 (ν _{1/2} = 700 Hz), 49.39 (ν _{1/2} = 240 Hz), 40.40 (ν _{1/2} = 180 Hz), 37.96 (s, 4H, ν _{1/2} = 37 Hz, H₁), 29.08 (s, 4H, ν _{1/2} = 40 Hz, H_m), 28.65 (ν _{1/2} = 250 Hz), 22.36 (ν _{1/2} = 120 Hz), 18.22 (s, 4H, ν _{1/2} = 24 Hz, H_m), 13.31 (s, 6H, ν _{1/2} = 17 Hz, H_o), -7.04 (s, 2H, ν _{1/2} = 20 Hz, H_e), -8.52 (ν _{1/2} = 430) Hz, -15.04 (s, 4H, ν _{1/2} = 24 Hz, H_d), -28.17 (ν _{1/2} = 120 Hz), -81.20 (ν _{1/2} = 340 Hz). IR (KBr Disk): ν (cm⁻¹) 3044.8, 2925.9, 2869.21, 1630.6, 1574.1, 1487.5, 1451.8, 1319.3, 1267.8, 1235.7, 1104.0, 1077.9, 1039.4, 1001.1, 936.5, 910.6, 848.6, 787.5, 726.9, 710.7. UV-Vis (nm, CH₂Cl₂): 664.1, 395.9. MALDI-TOF-TOF (Dithranol) (m/z): 1119.4 [M – 3Cl + Dithranol – 2H]⁺, 967.24 [M – Cl]⁺, 930.28 [M – 2Cl]⁺.

ESI/APCI-TOF HRA-MS (m/z): $[M-Cl]^+$ Calcd for $C_{50}H_{58}N_6Co_2Cl_3^+$ 967.2431; Found 967.2412. μ_{eff} (Evans Method): 6.3 BM.

(2)Fe₂Cl₄. FeCl₂ (136.5 mg, 1.077 mmol) and 2' (400.0 mg, 0.5383 mmol) were suspended in n-butanol (40 mL). The purple suspension was heated to 110 °C and stirred for 16 h, resulting in a dark blue solution. The solvent was evaporated and the crude solid suspended in Et₂O (10 mL). The crude solid was then collected by filtration, washed with THF (25 mL), and dried under vacuum to afford (2)Fe₂Cl₄ as a dark purple solid. The labelling scheme for (2)Fe₂Cl₄ is shown in Figure 9. ¹H NMR (CD₂Cl₂, 500 MHz): δ 139.3 (s, $v_{1/2}$ = 220 Hz), 134.3 (br s, $v_{1/2}$ = 370 Hz), 21.1 (br s, $v_{1/2} = 480$ Hz), 16.6 (s, $v_{1/2} = 92$ Hz), 12.2 (s, 4H, $v_{1/2} = 46$ Hz, H₁), 9.5 (s, $v_{1/2} = 98$ Hz), 6.7 (s, 2H, $v_{1/2} = 38$ Hz, H_e), 6.4 (s, 4H, $v_{1/2} = 46$ Hz, H_m), 2.1 (s, 4H, $v_{1/2} = 41$ Hz, H_n), 1.7 $(s, 6H, v_{1/2} = 37 \text{ Hz}, H_0), 1.5 (s, 4H, v_{1/2} = 59 \text{ Hz}, H_d), -4.9 (s, 4H, v_{1/2} = 98 \text{ Hz}), -20.6 (s, 4H, v_{1/2} = 98 \text{ Hz})$ = 130 Hz), -24.2 (s, 4H, $v_{1/2}$ = 110 Hz), -55.0 (s, 4H, $v_{1/2}$ = 150 Hz). IR (KBr Disk): $v(cm^{-1})$ 3048.8, 2953.2, 2930.2, 2868.6, 1625.8, 1572.8, 1487.3, 1452.8, 1426.1, 1377.1, 1320.4, 1283.9, 1270.2, 1236.5, 1199.3, 1149.3, 1102.4, 1076.9, 1039.7, 1001.8, 967.6, 929.5, 912.3, 876.3, 849.3, 786.5, 728.9, 708.8, 650.6, 622.7, 598.7. UV-Vis (nm, CH₂Cl₂): 612.1, 330.0. MALDI-TOF-TOF (Dithranol) (m/z): $1113.35 \text{ [M} - 3\text{Cl} + \text{Dithranol} - 2\text{H}]^+$, $961.25 \text{ [M} - \text{Cl}]^+$, 929.62 [M- 2Cl]⁺. ESI/APCI-TOF HRA-MS (m/z): [M-Cl]⁺ Calcd for C₅₀H₅₈N₆Fe₂Cl₃⁺ 961.2468; Found: 961.2498. μ_{eff} (Evans Method): 7.1 BM.

[(2)Pd₂Br₂][BAr^F₄]₂. PdBr₂ (477.4 mg, 1.794 mmol) and 2' (333.2 mg, 0.4484 mmol) were suspended in CH₃CN (40 mL). The orange suspension was stirred for 16 h at room temperature. The resulting brown solid was collected by filtration and washed with CH₃CN (40 mL). This solid was presumed to be [(2)Pd₂Br₂][Pd₂Br₆]₂. Yield: 700.0 mg, 88%. [(2)Pd₂Br₂][Pd₂Br₆]₂ (100.0 mg, 0.055 mmol) was suspended in CH₂Cl₂ (15 mL) and the mixture was stirred rapidly.

NaBAr^F₄ (98.0 mg, 0.111 mmol) was added in one portion and the suspension was stirred for 1 h at room temperature. The suspension was filtered through Celite and concentrated to ca. 5 mL. The concentrate was filtered through a 0.2 µm syringe filter and further concentrated to afford a dark brown solid, which was dried overnight under vacuum. The crude solid was triturated with Et₂O (15 mL) and the resulting pale brown solid was collected by filtration and dried under vacuum to yield [(2)Pd₂Br₂][BAr^F₄]₂. Yield: 80.1 mg, 51 %. The labelling scheme for $[(2)Pd_2Br_2][BAr^F_4]_2$ is shown in Figure 10. ¹H NMR (CD₂Cl₂, 500 MHz): δ 8.18 (s, 2H, H_c), 7.72 (br s, 16H, H_q), 7.56 (br s, 8H, H_p), 7.36 (t, ${}^{3}J_{HH} = 5$ Hz, 2H, H_e), 7.22 (d, ${}^{3}J_{HH} = 5$ Hz, 4H, H_d), 5.54 (br s, 4H, H_a), 4.69 (br s, 4H, H_b), 3.00 (br s, 4H, H_k), 2.87 (br s, 8H, H_f, H_g), 2.71 (br t, 4H, H_1), 2.60 (br s, 4H, H_1), 2.07 (br s, 8H, H_h , H_1), 1.42 (br s, 8H, H_m , H_n), 0.93 (br t, 6H, H_0). 13 C{ 1 H} NMR (CD₂Cl₂, 126 MHz): δ 184.7 (C=N), 162.1 (q, $^{1}J_{CB}$ = 50 Hz, C-B), 156.4 (p-py), 149.6 (*m*-py), 143.9 (*o*-py), 135.9 (C_{xylyl} - C_{benzylic}), 135.2 (C_{Hq}), 129.8 (C_{Hc}), 129.2 (qq, $^2J_{\text{CF}}$ = 31 Hz, ${}^{3}J_{CB} = 3$ Hz, C-CF₃), 129.0 (C-H_e), 125.0 (q, ${}^{1}J_{CF} = 270$ Hz, -CF₃), 128.2 (C-H_d), 117.9 $(m, C-H_p)$, 59.2 $(C-H_a,H_b)$, 30.8 $(C-H_k,H_i)$, 30.6 $(C-H_m)$, 29.4 $(C-H_l)$, 24.6 $(C-H_f,H_g)$, 23.3 $(C-H_b,H_g)$, 24.6 $(C-H_g,H_g)$, 25.3 $(C-H_g,H_g)$, 26.4 $(C-H_g,H_g)$, 26.5 $(C-H_g,H_g)$, 27.5 $(C-H_g,H_g)$, 27.5 $(C-H_g,H_g)$, 28.5 $(C-H_g,H_g)$, 29.4 $(C-H_g,H_g)$, 29.5 $(C-H_g,H_g)$, 29.5 $(C-H_g,H_g)$, 29.5 $(C-H_g,H_g)$, 29.5 $(C-H_g,H_g)$, 29.6 $(C-H_g,H_g)$, 29.6 $(C-H_g,H_g)$, 29.7 $(C-H_g,H_g)$, 29.7 $(C-H_g,H_g)$, 29.8 $(C-H_g,H_g)$ H_n), 21.9 (C- H_h , H_i), 13.7 (C- H_o). ¹⁹F{¹H} NMR (CD₂Cl₂, 470 MHz): δ -63.3. ¹¹B{¹H} NMR $(CD_2Cl_2, 128.4 \text{ MHz})$: δ -6.6. IR (KBr, Disk): $v(cm^{-1})$ 2965.1, 2879.0, 1653.4, 1610.2, 1569.4, 1457.2, 1355.23, 1278.4, 1121.1, 1001.1, 936.6, 886.8, 838.9, 785.7, 744.7, 712.15. ESI/APCI-TOF HRA-MS (m/z): $[M-BAr^{F_4}]^+$ Calcd for $C_{82}H_{70}BBr_2F_{24}N_6Pd_2^+$ 1979.1828; Found 1979.1829.

$$\begin{array}{c|c} & & & & \\ & & & & \\ & & & & \\ & & & \\ & & & \\ & & & \\ & & & \\ & & & \\ & & & \\ & & & \\ & & & \\ & & & \\ & &$$

Figure 10. Labelling scheme for [(2)Pd₂Br₂][BAr^F₄]₂.

(2'-4H)Zr₂(NMe₂)₄. Zr(NMe₂)₄ (222.1 mg, 0.8300 mmol) and 2' (308.4 mg, 0.4150 mmol) were suspended in PhCl (10 mL). The yellow suspension was stirred for 5 h at room temperature. Hexane (10 mL) was added and the yellow-orange suspension was stirred while being purged with N₂. The resulting bright yellow solid was collected by filtration, washed with hexane (2 x 25 mL) and dried under vacuum overnight to yield (2'-4H)Zr₂(NMe₂)₄. Yield: 360 mg, 79%. The labelling scheme for (2'-4H)Zr₂(NMe₂)₄ is shown in Figure 11. ¹H NMR (C₆D₆, 500 MHz): δ 8.11 (s, 2H, H_e), 7.27 (m, 6H, H_d, H_e), 5.40 (d, ²J_{HH} = 15 Hz, 4H, H_a), 4.79 (dd, ³J_{HH} = 5 Hz, ³J_{HH} = 8 Hz, 4H, H_j) 4.67 (d, ²J_{HH} = 15 Hz, 4H, H_b), 3.03 (s, 12H, NMe₂), 2.95 (s, 12H, NMe₂), 2.20 (m, 20 H, H_f, H_g, H_h, H_i, H_k), 1.04 (m, 8H, H₁, H_m), 0.77 (t, ³J_{HH} = 6.5 Hz, 6H, H_n). ¹H NMR (C₆D₅Cl, 500 MHz): δ 7.91 (s, 2H, H_c), 7.24 (t, J_{HH} = 7 Hz, 2H, H_c), 7.14 (d, H_d, overlapped with solvent resonance), 5.24 (d, ²J_{HH} = 15 Hz, 4H, H_a), 4.65 (dd, ³J_{HH} = 3 Hz, ³J_{HH} = 9 Hz, 4H, H_j) 4.54 (d, ²J_{HH} = 15 Hz, 4H, H_b), 2.96 (s, 12H, NMe₂), 2.78 (s, 12H, NMe₂), 2.17 (m, 20 H, H_f, H_g, H_h, H_i, H_k), 1.09 (m, 8H, H₁, H_m), 0.81 (t, ³J_{HH} = 7 Hz, 6H, H_n). ¹³C{¹H} NMR (C₆D₅Cl, 126 MHz): δ 151.2 (py-o), 148.6 (py-p), 148.4 (C_{xylyl}-C_{benzylic}), 143.6 (py-m), 127.2 (C-H_d), 126.7

(obscured by solvent resonances, from HSQC, C-H_e), 125.9 (obscured by solvent resonances, from HSQC, C-H_c), 98.4 (C-H_j), 53.6 (C-H_a,H_b), 43.3 (N-CH₃), 42.1 (N-CH₃), 30.9 (C-H_l or C-H_m), 27.8 (C-H_k), 23.5 (C-H_h,H_i), 23.0 (C-H_f,H_g), 22.9 (C-H_l or C-H_m), 14.1 (C-H_n); the N-C=C ¹³C NMR resonance is obscured by solvent resonances. Anal. Calcd for C₅₈H₇₈N₁₀Zr₂: C, 63.46; H, 7.16; N, 12.76. Found: C, 63.22; H, 7.35; N, 12.42.

Figure 11. Labelling scheme for (2'–4H)Zr₂(NMe₂)₄, (2'–4H)Zr₂Me₄ and (2'–4H)Zr₂(CH₂SiMe₃)₂(NMe₂)₂

(2'-4H)Zr₂Me₄. (2'-4H)Zr₂(NMe₂)₄ (300.0 mg, 0.2733 mmol) was suspended in benzene (30 mL), the mixture was stirred, and AlMe₃ (394.0 mg, 2.733 mmol) was added dropwise. The mixturewas stirred for 16 h at room temperature. Hexane (30 mL) was added and the suspension was filtered. The resulting solid was washed with hexane (15 mL), Et₂O (2 x 10 mL), and hexane (15 mL) and dried overnight to yield (2'-4H)Zr₂Me₄ as a bright yellow solid which contains 10 % Et₂O by ¹H NMR. Yield 180.3 mg, 67 %. The labelling scheme for (2'-4H)Zr₂Me₄ is shown in Figure 11. ¹H NMR (C₆D₆, 500 MHz, 23 °C): δ 8.45 (s, 2H, H_c), 7.33 (t, ³J_{HH} = 7.5 Hz, 2H,

 H_e), 7.25 (d, ${}^3J_{HH}$ = 7.5 Hz, 2H, H_d), 5.59 (d, ${}^2J_{HH}$ = 15 Hz, 4H, H_a), 4.82 (t, ${}^3J_{HH}$ = 4 Hz, 4H, H_j) 4.61 (d, ${}^2J_{HH}$ = 15 Hz, 4H, H_b), 2.2 (m, 12H, H_f , H_g , H_h , H_i), 2.03 (t, 4H, H_k), 1.06 (m, 20 H, H_l , H_m), 0.76 (t, ${}^3J_{HH}$ = 7 Hz, 6H, H_n), 0.57 (s, 6H, Zr- Me^1), 0.55 (s, 6H, Zr- Me^2). Anal. Calcd for $C_{54}H_{66}N_6Zr_2$: C_{7} , 66.07; H_{7} , 6.78; N_{7} , 8.56. Found: C_{7} , 65.56; C_{7} , 7.18; C_{7} , 8.34.

Notes: This compound decomposes instantly upon exposure to chlorinated solvents and is not soluble enough in C_6D_6 or $C_6D_5CD_3$ for a ^{13}C NMR spectrum to be collected. The sample used for elemental analysis was placed under vacuum for 24 h to remove the residual Et_2O . The deviation in the %C from the \pm 0.4% standard may be due to formation of Zr-carbide during combustion.

(2'-4H)Zr₂(CH₂SiMe₃)₂(NMe₂)₂. (2'-4H)Zr₂(NMe₂)₄ (296.9 mg, 0.2850 mmol) was suspended in PhMe (15 mL) and Al(CH₂SiMe₃)₃ (411.2 mg, 1.425) was added in one portion. The mixture was heated at 80 °C and stirred for 16 h. The solvent was removed under reduced pressure. The resulting dark yellow solid was suspended in Et₂O (15 mL) and stirred for 5 min. Pentane (15 mL) was added, the suspension was filtered, and the solid washed with pentane (2 x 15 mL) and dried under vacuum overnight to yield (2'-4H)Zr₂(CH₂SiMe₃)₂(NMe₂)₂ as a dark yellow solid. Yield: 250.0 mg, 74 %. The labelling scheme for (2'-4H)Zr₂(CH₂SiMe₃)₂(NMe₂)₂ is shown in Figure 11. ¹H NMR (C₆D₆, 500 MHz): δ 7.88 (s, 2H, H_c), 7.24 (t, J_{HH} = 7.5 Hz, 2H, H_c), 7.17 (d, J_{HH} = 7.5 Hz, H_d, overlapped with solvent peak) 5.37 (t, ² J_{HH} = 15 Hz, 4H, H_a), 4.83 (br dd, 4H, H_j), 4.69 (d, ² J_{HH} = 15 Hz, 4H, H_b), 2.79 (s, 12H, -N(CH₃)₂), 2.35 (m, 8 H, H_f, H_g), 2.13 (m, 12H, H_h, H_i, H_k), 1.07 (m, 8H, H_I, H_m), 0.78 (t, 6H, H_n, ³ J_{HH} = 6 Hz), 0.72 (s, 4H, -CH₂Si(CH₃)₃), 0.02 (s, 18H, -CH₂Si(CH₃)₃). ¹³C{¹H} NMR (C₆D₆, 126 MHz): δ 151.3 (*o*-py), 149.2 (*p*-py), 148.7 (*C*_{xylyl}-C_{benzylic}), 143.56 (*m*-py), 127.6 (*C*-H_d), 126.9 (*C*-H_e), 126.0 (*C*-H_e),

99.7 (*C*-H_i), 53.7 (*C*-H_a,H_b), 51.1 (-*CH*₂Si(CH₃)₃), 41.1 (-*N*(*C*H₃)₂), 31.0 (*C*-H_l), 27.9 (*C*-H_k), 23.6 (*C*-H_h,H_i), 23.3 (*C*-H_f,H_g), 22.9 (*C*-H_m), 14.1 (*C*-H_n), 2.5 (-*CH*₂Si(*CH*₃)₃); the *N*-*C*=*C* ¹³*C* NMR resonance is obscured by solvent resonances. Anal. Calcd for C₆₂H₈₈N₈Si₂Zr₂: C, 62.89; H, 7.49; N, 9.46. Found: C, 62.61; H, 7.50; N, 9.47.

ASSOCIATED CONTENT

Supporting Information. The supporting Information is available free of charge on the ACS Publications website.

NMR and mass spectra for compounds, explanation of NMR assignments for (2)Zn2Cl4, variable temperature NMR proce-dures and analysis, X-ray crystallographic details, and conformational analysis (PDF)

Accession Codes. CCDC 1872094 ((2)Co₂Cl₄), 1872095 ([(2)Pd₂Br₂][BAr^F₄]₂), 1872096 ((2)Zn₂Cl₄), 1917919 ((2'-4H)Zr₂(CH₂SiMe₃)₂(NMe₂)₂) contain the supplementary crystallographic data for this paper. These data can be obtained free of charge via www.ccdc.cam.ac.uk/data_request/cif, or by emailing data_request@ccdc.cam.ac.uk, or by contacting The Cambridge Crystallographic Data Centre, 12, Union Road, Cambridge CB2 1EZ, UK; fax: +44 1223 336033

AUTHOR INFORMATION

Corresponding Author

*rfjordan@uchicago.edu

ORCID

Erik D. Reinhart: <u>0000-0003-2878-9376</u>

Richard F. Jordan: 0000-0002-3158-4745

Funding Sources

This work was supported by the National Science Foundation (NSF) under grant CHE-1709159.

Notes

The authors declare no competing financial interest.

ACKNOWLEDGMENT

We thank Dr. Antoni Jurkiewicz for assistance with NMR, Dr. Alexander Filatov and Andrew

McNeece for X-ray crystallography, and Dr. Chang Qin mass spectrometry.

REFERENCES

(1) Small, B. L.; Brookhart, M.; Bennett, A. M. A. Highly Active Iron and Cobalt Catalysts

for the Polymerization of Ethylene. J. Am. Chem. Soc. 1998, 120, 4049–4050.

(2) Small, B. L. Discovery and Development of Pyridine-bis(imine) and Related Catalysts for

Olefin Polymerization and Oligomerization. Acc. Chem. Res. 2015, 48, 2599–2611.

(3) Britovsek, G. J. P.; Bruce, M.; Gibson, V. C.; Kimberley, B. S.; Maddox, P. J.;

Mastroianni, S.; McTavish, S. J.; Redshaw, C.; Solan, G. A.; Strömberg, S.; White, A. J.;

Williams, D. J. Iron and Cobalt Ethylene Polymerization Catalysts Bearing 2,6-

Bis(Imino)Pyridyl Ligands: Synthesis, Structures, and Polymerization Studies. J. Am.

Chem. Soc. 1999, 121, 8728-8740.

37

- (4) Gibson, V. C.; Redshaw, C.; Solan, G. A. Bis(imino)pyridines: Surprisingly Reactive Ligands and a Gateway to New Families of Catalysts. *Chem. Rev.* **2007**, *107*, 1745–1776.
- (5) Flisak, Z.; Sun, W.-H. Progression of Diiminopyridines: From Single Application to Catalytic Versatility. *ACS Catal.* **2015**, *5*, 4713–4724.
- (6) Biernesser, A. B.; Li, B.; Byers, J. A. Redox-controlled Polymerization of Lactide Catalyzed by Bis(imino)pyridine Iron Bis(alkoxide) Complexes. *J. Am. Chem. Soc.* **2013**, *135*, 16553–16560.
- (7) Qi, M.; Dong, Q.; Wang, D.; Byers, J. A. Electrochemically Switchable Ring-Opening Polymerization of Lactide and Cyclohexene Oxide. *J. Am. Chem. Soc.* **2018**, *140*, 5686–5690.
- (8) Schmidt, V. A.; Hoyt, J. M.; Margulieux, G. W.; Chirik, P. J. Cobalt-Catalyzed $[2\pi + 2\pi]$ Cycloadditions of Alkenes: Scope, Mechanism, and Elucidation of Electronic Structure of Catalytic Intermediates. *J. Am. Chem. Soc.* **2015**, *137*, 7903–7914.
- (9) Hoyt, J. M.; Schmidt, V. A.; Tondreau, A. M.; Chirik, P. J. Iron-catalyzed Intermolecular [2+2] Cycloadditions of Unactivated Alkenes. *Science* **2015**, *349*, 960–963.
- (10) Yang, X.; Wang, Z.-X. Mono- and Dinuclear Pincer Nickel Catalyzed Activation and Transformation of C–Cl, C–N, and C–O Bonds. *Organometallics* **2014**, *33*, 5863–5873.
- (11) Radlauer, M. R.; Day, M. W.; Agapie, T. Bimetallic Effects on Ethylene Polymerization in the Presence of Amines: Inhibition of the Deactivation by Lewis Bases. *J. Am. Chem. Soc.* **2012**, *134*, 1478–1481.

- (12) Mankad, N. P. Selectivity Effects in Bimetallic Catalysis. *Chem. Eur. J* **2016**, *22*, 5822–5829.
- (13) Thevenon, A.; Romain, C.; Bennington, M. S.; White, A. J. P.; Davidson, H. J.; Brooker, S.; Williams, C. K. Dizinc Lactide Polymerization Catalysts: Hyperactivity by Control of Ligand Conformation and Metallic Cooperativity. *Angew. Chem. Int. Ed. Engl.* 2016, 55, 8680–8685.
- (14) Mazzacano, T. J.; Mankad, N. P. Base Metal Catalysts for Photochemical C-H Borylation That Utilize Metal-metal Cooperativity. *J. Am. Chem. Soc.* **2013**, *135*, 17258–17261.
- (15) Takeuchi, D.; Iwasawa, T.; Osakada, K. Double-Decker-Type Dipalladium Catalysts for Copolymerization of Ethylene with Acrylic Anhydride. *Macromolecules* **2018**, *51*, 5048–5054.
- (16) Rong, C.; Wang, F.; Li, W.; Chen, M. Ethylene Polymerization by Dinuclear Xanthene-Bridged Imino- and Aminopyridyl Nickel Complexes. *Organometallics* **2017**, *36*, 4458–4464.
- (17) Torkelson, J. R.; Antwi-Nsiah, F. H.; McDonald, R.; Cowie, M.; Pruis, J. G.; Jalkanen, K. J.; DeKock, R. L. Metal-metal Cooperativity Effects in Promoting C-H Bond Cleavage of a Methyl Group by an Adjacent Metal Center. J. Am. Chem. Soc. 1999, 121, 3666–3683.
- (18) Li, H.; Marks, T. J. Nuclearity and Cooperativity Effects in Binuclear Catalysts and Cocatalysts for Olefin Polymerization. *Proc. Natl. Acad. Sci. USA* **2006**, *103*, 15295–15302.

- (19) Gramigna, K. M.; Dickie, D. A.; Foxman, B. M.; Thomas, C. M. Cooperative H₂ Activation Across a Metal-Metal Multiple Bond and Hydrogenation Reactions Catalyzed by a Zr/Co Heterobimetallic Complex. *ACS Catal.* **2019**, *9*, 3453-3164.
- (20) McInnis, J. P.; Delferro, M.; Marks, T. J. Multinuclear Group 4 Catalysis: Olefin Polymerization Pathways Modified by Strong Metal-metal Cooperative Effects. Acc. Chem. Res. 2014, 47, 2545–2557.
- (21) Delferro, M.; Marks, T. J. Multinuclear Olefin Polymerization Catalysts. *Chem. Rev.* **2011**, *111*, 2450–2485.
- (22) Moore, D. R.; Cheng, M.; Lobkovsky, E. B.; Coates, G. W. Mechanism of the Alternating Copolymerization of Epoxides and CO₂ Using Beta-diiminate Zinc Catalysts: Evidence for a Bimetallic Epoxide Enchainment. *J. Am. Chem. Soc.* **2003**, *125*, 11911–11924.
- (23) Thomas, R. M.; Widger, P. C. B.; Ahmed, S. M.; Jeske, R. C.; Hirahata, W.; Lobkovsky,
 E. B.; Coates, G. W. Enantioselective Epoxide Polymerization Using a Bimetallic Cobalt
 Catalyst. J. Am. Chem. Soc. 2010, 132, 16520–16525.
- (24) Getzler, Y. D. Y. L.; Mahadevan, V.; Lobkovsky, E. B.; Coates, G. W. Stereochemistry of Epoxide Carbonylation Using Bimetallic Lewis Acid/metal Carbonyl Complexes. *Pure Appl. Chem.* **2004**, *76*, 557–564.
- (25) Morris, L. S.; Childers, M. I.; Coates, G. W. Bimetallic Chromium Catalysts with Chain Transfer Agents: A Route to Isotactic Poly(propylene Oxide)s with Narrow Dispersities. *Angew. Chem. Int. Ed. Engl.* **2018**, *57*, 5731–5734.

- (26) Widger, P. C. B.; Ahmed, S. M.; Coates, G. W. Exploration of Cocatalyst Effects on a Bimetallic Cobalt Catalyst System: Enhanced Activity and Enantioselectivity in Epoxide Polymerization. *Macromolecules* 2011, 44, 5666–5670.
- (27) Ahmed, S. M.; Poater, A.; Childers, M. I.; Widger, P. C. B.; LaPointe, A. M.; Lobkovsky, E. B.; Coates, G. W.; Cavallo, L. Enantioselective Polymerization of Epoxides Using Biaryl-linked Bimetallic Cobalt Catalysts: a Mechanistic Study. *J. Am. Chem. Soc.* 2013, 135, 18901–18911.
- (28) Takeuchi, D.; Takano, S.; Takeuchi, Y.; Osakada, K. Ethylene Polymerization at High Temperatures Catalyzed by Double-Decker-Type Dinuclear Iron and Cobalt Complexes: Dimer Effect on Stability of the Catalyst and Polydispersity of the Product. Organometallics 2014, 33, 5316–5323.
- (29) Takano, S.; Takeuchi, Y.; Takeuchi, D.; Osakada, K. Selective Formation of Ethyl-And/or Propyl-branched Oligoethylene Using Double-decker-type Dinuclear Fe Complexes as the Catalyst. *Chem. Lett.* **2014**, *43*, 465–467.
- (30) Liu, J.; Li, Y.; Liu, J.; Li, Z. Ethylene Polymerization with a Highly Active and Long-Lifetime Macrocycle Trinuclear 2,6-Bis(imino)pyridyliron. *Macromolecules* **2005**, *38*, 2559–2563.
- (31) Tolstikov, G. A.; Ivanchev, S. S.; Oleinik, I. I.; Ivancheva, N. I.; Oleinik, I. V. New Multifunctional Bis(imino)pyridine-Iron Chloride Complexes and Ethylene Polymerization Catalysts on Their Basis. *Dokl. Phys. Chem.* **2005**, *404*, 182–185.

- (32) Seitz, M.; Alt, H. G. Transition Metal Complexes of Polymeric Schiff Bases as Catalyst Precursors for the Polymerization of Ethylene. *J. Mol. Catal. A: Chem* **2006**, *257*, 73–77.
- (33) Wang, L.; Sun, J. Methylene Bridged Binuclear Bis(imino)pyridyl iron(II) Complexes and Their Use as Catalysts Together with Al(i-Bu)₃ for Ethylene Polymerization. *Inorg. Chim. Acta* **2008**, *361*, 1843–1849.
- (34) Suo, H.; Solan, G. A.; Ma, Y.; Sun, W.-H. Developments in Compartmentalized Bimetallic Transition Metal Ethylene Polymerization Catalysts. *Coord Chem. Rev.* **2018**, *372*, 101–116.
- (35) Xing, Q.; Zhao, T.; Qiao, Y.; Wang, L.; Redshaw, C.; Sun, W.-H. Synthesis, Characterization and Ethylene Polymerization Behavior of Binuclear Iron Complexes Bearing N,N'-bis(1-(6-(1-(arylimino)ethyl) Pyridin-2-yl)ethylidene)benzidines. *RSC Adv.* **2013**, *3*, 26184.
- (36) Xing, Q.; Zhao, T.; Du, S.; Yang, W.; Liang, T.; Redshaw, C.; Sun, W.-H. Biphenyl-Bridged 6-(1-Aryliminoethyl)-2-iminopyridylcobalt Complexes: Synthesis, Characterization, and Ethylene Polymerization Behavior. *Organometallics* **2014**, *33*, 1382–1388.
- (37) Rezaeivala, M.; Keypour, H. Schiff Base and non-Schiff Base Macrocyclic Ligands and Complexes Incorporating the Pyridine Moiety The First 50 Years. *Coord Chem. Rev.* **2014**, *280*, 203–253.

- (38) Healy, M. D. S.; Rest, A. J. Template Reactions. In *Advances in Inorganic Chemistry and Radiochemistry*; Emeléus H. J.; Sharpe, A. G., Eds.; Academic Press: New York, 1978; Vol. 21, pp. 1–40.
- (39) Cabbiness, D. K.; Margerum, D. W. Macrocyclic Effect on the Stability of copper(II) Tetramine Complexes. *J. Am. Chem. Soc.* **1969**, *91*, 6540–6541.
- (40) Izatt, R. M.; Christensen, J. J., Eds.; Synthesis of Macrocycles: The Design of Selective Complexing Agents (Progress in Macrocyclic Chemistry), Vol. 3; 1st ed.; Wiley: New York, 1987.
- (41) Izatt, R. M.; Christensen, J. J., Eds.; *Synthetic Multidentate Macrocyclic Compounds*; Academic Press: New York, 1978.
- (42) Busch, D. H.; Stephenson, N. A. Molecular Organization, Portal to Supramolecular chemistry. Structural Analysis of the Factors Associated with Molecular Organization in Coordination and Inclusion Chemistry, Including the Coordination Template Effect. Coord Chem. Rev. 1990, 100, 119–154.
- (43) Curtis, N. F. Macrocyclic Coordination Compounds Formed by Condensation of Metalamine Complexes with Aliphatic Carbonyl Compounds. *Coord Chem. Rev.* **1968**, *3*, 3–47.
- (44) Costisor, O.; Linert, W. *Metal Mediated Template Synthesis of Ligands*; World Scientific Singapore: Singapore, 2004.
- (45) Thompson, M. C.; Busch, D. H. Reactions of Coordinated Ligands. VI. Metal Ion Control in the Synthesis of Planar Nickel(II) Complexes of α-Diketo-bis-mercaptoimines. J. Am. Chem. Soc. 1964, 86, 213–217.

- (46) Salata, C. A.; Youinou, M. T.; Burrows, C. J. (Template)2 Synthesis of a Dinucleating Macrocyclic Ligand and Crystal Structure of its Dicopper(II) Imidazolate Complex. J. Am. Chem. Soc. 1989, 111, 9278–9279.
- (47) Salata, C. A.; Youinou, M. T.; Burrows, C. J. Preparation and Structural Characterization of Dicopper(II) and Dinickel(II) Imidazolate-bridged Macrocyclic Schiff Base Complexes. *Inorg. Chem.* **1991**, *30*, 3454–3461.
- (48) Drew, M. G. B.; Cairns, C.; Lavery, A.; Nelson, S. M. Binuclear copper(II) Complexes of a 24-membered Macrocyclic Schiff Base Ligand Containing Intramolecularly Bound Substrate Molecules and Ions: X-ray Structure of a μ-imidazolate Complex. *J. Chem. Soc., Chem. Commun.* **1980**, 1122–1124.
- (49) Beattie, J. W.; SantaLucia, D. J.; White, D. S.; Groysman, S. Oxalate-templated Synthesis of Di-zinc Macrocycles. *Inorg. Chim. Acta* **2017**, *460*, 8–16.
- (50) Browne, C.; Ronson, T. K.; Nitschke, J. R. Palladium-templated Subcomponent Self-assembly of Macrocycles, Catenanes, and Rotaxanes. *Angew. Chem. Int. Ed. Engl.* **2014**, *53*, 10701–10705.
- (51) Dammann, W.; Buban, T.; Schiller, C.; Burger, P. Dinuclear Tethered Pyridine, Diimine Complexes. *Dalton Trans.* **2018**, *47*, 12105–12117.
- (52) Huang, F.; Xing, Q.; Liang, T.; Flisak, Z.; Ye, B.; Hu, X.; Yang, W.; Sun, W.-H. 2-(1-Aryliminoethyl)-9-arylimino-5,6,7,8-tetrahydrocycloheptapyridyl iron(II) Dichloride: Synthesis, Characterization, and the Highly Active and Tunable Active Species in Ethylene Polymerization. *Dalton Trans.* **2014**, *43*, 16818–16829.

- (53) Agrifoglio, G.; Reyes, J.; Atencio, R.; Briceño, A. 2,6-Bis[1-(2-isopropyl-phenyl-imino)-ethyl]-pyridine. *Acta Crystallogr. Sect. E, Struct. Rep. Online* **2007**, *64*, o28–o29.
- (54) Wallenhorst, C.; Kehr, G.; Luftmann, H.; Fröhlich, R.; Erker, G. Bis(iminoethyl)pyridine Systems with a Pendant Alkenyl Group. Part A: Cobalt and Iron Complexes and Their Catalytic Behavior. *Organometallics* **2008**, *27*, 6547–6556.
- (55) Ionkin, A. S.; Marshall, W. J.; Adelman, D. J.; Fones, B. B.; Fish, B. M.; Schiffhauer, M. F.; Soper, P. D.; Waterland, R. L.; Spence, R. E.; Xie, T. High-temperature Catalysts for the Production of α-olefins Based on Iron(II) and Iron(III) Tridentate Bis(imino)pyridine Complexes Modified by Nitrilo Group. *J. Polym. Sci. A Polym. Chem.* 2008, 46, 585–611.
- (56) Pelascini, F.; Wesolek, M.; Peruch, F.; Lutz, P. J. Modified Pyridine-Bis(imine) Iron and Cobalt Complexes: Synthesis, Structure, and Ethylene Polymerization Study. *Eur. J. Inorg. Chem.* **2006**, 4309–4316.
- (57) Thummel, R. P.; Jahng, Y. Polyaza Cavity Shaped Molecules. 4. Annelated Derivatives of 2,2':6',2"-terpyridine. *J. Org. Chem.* **1985**, *50*, 2407–2412.
- (58) Appukuttan, V. K.; Liu, Y.; Son, B. C.; Ha, C.-S.; Suh, H.; Kim, I. Iron and Cobalt Complexes of 2,3,7,8-Tetrahydroacridine-4,5(1*H* ,6*H*)-diimine Sterically Modulated by Substituted Aryl Rings for the Selective Oligomerization to Polymerization of Ethylene. *Organometallics* **2011**, *30*, 2285–2294.
- (59) Hanton, M. J.; Tenza, K. Bis(imino)pyridine Complexes of the First-Row Transition Metals: Alternative Methods of Activation. *Organometallics* **2008**, *27*, 5712–5716.

- (60) Bell, T. W.; Rothenberger, S. D. Synthesis of Annelated Pyridines from 1,5-diketone Equivalents Using Cupric Acetate and Ammonium Acetate. *Tetrahedron Lett.* **1987**, *28*, 4817–4820.
- Bell, T. W.; Cho, Y.-M.; Firestone, A.; Karin, H.; Liu, J.; Ludwig, R.; Rothenberger, S.
 D. 9-n-BUTYL-1,2,3,4,5,6,7,8-OCTAHYDROACRIDIN-4-OL. *Org. Synth.* 1990, 69, 226.
- (62) Pilato, M. L.; Catalano, V. J.; Bell, T. W. Synthesis of 1,2,3,4,5,6,7,8-Octahydroacridine via Condensation of Cyclohexanone with Formaldehyde. *J. Org. Chem.* **2001**, *66*, 1525–1527.
- (63) Groen, J. H.; Annemieke, de Z.; Vlaar, M. J. M.; Ernsting, J. M.; van Leeuwen, P. W. N. M.; Vrieze, K.; Kooijman, H.; Smeets, W. J. J.; Spek, A. L.; Budzelaar, P. H. M.; Qin, X.; Thummel, R. P. Insertion Reactions into Palladium–Carbon Bonds of Complexes Containing Terdentate Nitrogen Ligands; Experimental and Ab Initio MO Studies. *Eur. J. Inorg. Chem.* 1998, 1129-1143.
- (64) Li, X.; Zhu, D.; Gao, W.; Zhang, Y.; Mu, Y. Synthesis, Structures and Luminescent Properties of [ZnCl₂(2,6-bis{1-(phenylimino)ethyl}pyridine)]. *J. Chem. Res.* **2006**, *2006*, 371–373.
- (65) Fan, R.; Zhu, D.; Ding, H.; Mu, Y.; Su, Q.; Xia, H. Blue Luminescent zinc(II) Complexes of 2,6-bis[1-(2,6-diisopropylphenylimino)ethyl]pyridine and 2,6-bis[1-(2,6-dimethylphenylimino)ethyl]pyridine. *Synth. Met.* **2005**, *149*, 135–141.

- (66) Blahut, J.; Hermann, P.; Tošner, Z.; Platas-Iglesias, C. A Combined NMR and DFT Study of Conformational Dynamics in Lanthanide Complexes of Macrocyclic DOTA-like Ligands. *Phys. Chem. Chem. Phys.* **2017**, *19*, 26662–26671.
- (67) Klawitter, I.; Anneser, M. R.; Dechert, S.; Meyer, S.; Demeshko, S.; Haslinger, S.; Pöthig, A.; Kühn, F. E.; Meyer, F. Iron Complexes of a Macrocyclic N-Heterocyclic Carbene/Pyridine Hybrid Ligand. *Organometallics* 2015, 34, 2819–2825.
- (68) Bogdan, A. R.; Jerome, S. V.; Houk, K. N.; James, K. Strained Cyclophane Macrocycles: Impact of Progressive Ring Size Reduction on Synthesis and Structure. *J. Am. Chem. Soc.* 2012, 134, 2127–2138.
- (69) Weber, B.; Kaps, E. Synthesis and Magnetic Properties of New Dinuclear iron(II) Complexes of a Phenylene-bridge Shiff Base Analogue Dinucleating Ligand. *Heteroatom Chem.* **2005**, *16*, 391–397.
- (70) Hossain, M. J.; Yamasaki, M.; Mikuriya, M.; Kuribayashi, A.; Sakiyama, H. Synthesis, Structure, and Magnetic Properties of Dinuclear Cobalt(II) Complexes with a New Phenol-Based Dinucleating Ligand with Four Hydroxyethyl Chelating Arms. *Inorg. Chem.* **2002**, *41*, 4058–4062.
- (71) Dayan, O.; Doĝan, F.; Kaya, İ.; Çetinkaya, B. Palladium(II) Complexes Containing 2,6-Bis(Imino)Pyridines: Synthesis, Characterization, Thermal Study, and Catalytic Activity in Suzuki Reactions. *Synth. React. Inorg. Met.-Org. Chem.* **2010**, *40*, 337–344.
- (72) Liu, P.; Zhou, L.; Li, X.; He, R. Bis(imino)pyridine Palladium(II) Complexes: Synthesis, Structure and Catalytic Activity. *J. Organomet. Chem.* **2009**, *694*, 2290–2294.

- (73) Jurca, T.; Hiscock, L. K.; Korobkov, I.; Rowley, C. N.; Richeson, D. S. The Tipping Point of the Inert Pair Effect: Experimental and Computational Comparison of In(I) and Sn(II) Bis(imino)pyridine Complexes. *Dalton Trans.* **2014**, *43*, 690–697.
- (74) Singh, A. P.; Roesky, H. W.; Carl, E.; Stalke, D.; Demers, J.-P.; Lange, A. Lewis Base Mediated Autoionization of GeCl₂ and SnCl₂. *J. Am. Chem. Soc.* **2012**, *134*, 4998–5003.
- (75) Tušek-Božić, L.; Matijašić, I.; Bocelli, G.; Sgarabotto, P.; Furlani, A.; Scarcia, V.; Papaioannou, A. Preparation, Characterization and Activity of Palladium(II) Halide Complexes with Diethyl 8-quinolylmethylphosphonate (8-dqmp). X-ray Crystal Structure of [8-dqmpH]₂[PdCl₄]·2H₂O and [8-dqmpH]₂[Pd₂Br₆]. *Inorg. Chim. Acta* **1991**, *185*, 229–237.
- (76) Moreno-Vida, M. I.; Colacio-Rodriguez, E.; Moreno-Carretero, M. N.; Salas-Peregrin, J. M.; Simard, M.; Beauchamp, A. L. Bromopalladates(II) of Xanthine Derivatives. Crystal Structure of 1,3,8-trimethylxanthinium tribromopalladate(II) Monohydrate. *Inorg. Chim. Acta* 1989, 157, 201–207.
- (77) Naghipour, A.; Ghorbani-Choghamarani, A.; Heidarizadi, F.; Notash, B. Synthesis, Characterization and Structural Study of a Phosphonium Salt Containing the [Pd₂Br₆]²⁻ Ion and Its Application as a Novel, Efficient and Renewable Heterogeneous Catalyst for Amination of Aryl Halides and the Stille Cross-coupling Reaction. *Polyhedron* **2016**, *105*, 18–26.
- (78) Reardon, D.; Aharonian, G.; Gambarotta, S.; Yap, G. P. A. Mono- and Zerovalent Manganese Alkyl Complexes Supported by the α,α'-Diiminato Pyridine Ligand: Alkyl

- Stabilization at the Expense of Catalytic Performance. *Organometallics* **2002**, *21*, 786–788.
- (79) Sugiyama, H.; Korobkov, I.; Gambarotta, S.; Möller, A.; Budzelaar, P. H. M. Preparation, Characterization, and Magnetic Behavior of the Ln Derivatives (ln = Nd, La) of a 2,6-diminepyridine Ligand and Corresponding Dianion. *Inorg. Chem.* **2004**, *43*, 5771–5779.
- (80) Bouwkamp, M. W.; Lobkovsky, E.; Chirik, P. J. Bis(imino)pyridine Ligand Deprotonation Promoted by a Transient Iron Amide. *Inorg. Chem.* **2006**, *45*, 2–4.
- (81) Beachley, O. T.; Tessier-Youngs, C.; Simmons, R. G.; Hallock, R. B. Attempted Syntheses of Low-oxidation-state Organometallic Derivatives of Aluminum, Gallium, and Indium. A New Synthesis of Tris(trimethylsilylmethyl)aluminum (Al(CH₂SiMe₃)₃). *Inorg. Chem.* **1982**, *21*, 1970–1973.
- (82) Loos, M.; Gerber, C.; Corona, F.; Hollender, J.; Singer, H. Accelerated Isotope Fine Structure Calculation Using Pruned Transition Trees. *Anal. Chem.* **2015**, *87*, 5738–5744.

SYNOPSIS

An octahydro-4,5-acridinedione was used to synthesize a macrocyclic bis(pyridine-dienamine) proligand. The synthesis and characterization of dinuclear complexes supported by bis(pyridine-dienamido) ligands are described.

TOC GRAPHIC

Template-Free Synthesis
bis-PDI and bis-PDE Dinuclear Complexes